Limits and constraints on mechanisms of cell-cycle regulation imposed by cell size-homeostasis measurements

Lisa Willis[1,*], Henrik Jönsson[2,3], Kerwyn Casey Huang[1,4,5,*]

[1]Department of Bioengineering, Stanford University, Stanford, CA 94305, USA

[2]Sainsbury Laboratory, University of Cambridge, Cambridge, CB2 1LR, UK

[3]Department of Applied Mathematics and Theoretical Physics, University of Cambridge, Cambridge, CB3 0DZ, UK

[4]Department of Microbiology and Immunology, Stanford University, Stanford, CA 94305, USA

[5]Chan Zuckerberg Biohub, San Francisco, CA 94158, USA

*Correspondence: lisawillis@stanford.edu, kchuang@stanford.edu

Lead contact: kchuang@stanford.edu

Summary

High-throughput imaging has led to an explosion of observations regarding cell-size homeostasis across the kingdoms of life. Among bacteria, "adder" behavior in which a constant size appears to be added during each cell cycle is ubiquitous, while various eukaryotes show other size-homeostasis behaviors. Since interactions between cell-cycle progression and growth ultimately determine size-homeostasis behaviors, we developed a general model of cell-cycle regulation. Our analyses revealed a range of scenarios that are plausible yet nevertheless fail to regulate cell size, indicating that mechanisms of cell-cycle regulation are stringently limited by size-control requirements and possibly why certain cell-cycle features are strongly conserved. Cell-cycle features can play unintuitive roles in altering size homeostasis behaviors: noisy regulator production can enhance adder behavior, while Whi5-like inhibitor dilutors respond sensitively to perturbations to G2/M control and noisy G1/S checkpoints. The model thus provides holistic insight into the mechanistic implications of cell-size homeostasis measurements.

Keywords: *Cell-size homeostasis, cell growth, cell-cycle checkpoints, CDK1-cyclin activity, Whi5, FtsZ, DnaA, inhibitor dilutor, mechanistic models, phenomenological models*

Introduction

One of the most fundamental questions in biology is how cells regulate cell-cycle progression, which is intimately tied to myriad processes such as cell-size determination (Schmoller et al., 2015), drug sensitivity (Shi et al., 2017), and transcription (Padovan-Merhard et al., 2015). In all organisms, cell-cycle control must be coupled to growth to ensure cell-size homeostasis, the maintenance of a fixed average size in steady-state conditions. Measurable size-homeostasis behaviors are determined by interactions between cell-cycle control and growth. Single-cell lineage tracking and cell-cycle reporters have led to a rapid proliferation in size homeostasis measurements across bacteria, yeast, mammalian cells, and plant cells. Among bacteria (Campos et al., 2014; Taheri-Araghi et al., 2015; Wallden et al., 2016; Willis and Huang, 2017) and an archaeon (Eun et al., 2018), a common theme has emerged: cells appear to regulate their size via an "adder" behavior whereby a fixed volume is added between birth and division. Among eukaryotes, budding yeast and mammalian cells can deviate from adder behavior over the G1 and S/G2 cell-cycle stages while maintaining apparent adder or near-adder behavior between birth and division (Cadart et al., 2018; Chandler-Brown et al., 2017; Di Talia et al., 2007; Schmoller et al., 2015), with the smallest mammalian cells switching to approximately "sizer" behavior with no correlation between birth and division sizes (Varsano et al., 2017). Similarly, small fission yeast cells exhibit sizer behavior at division while large fission yeast cells exhibit near-adder

behavior (Facchetti et al., 2019; Fantes, 1977; Pan et al., 2014). By contrast, stem cells of *Arabidopsis thaliana* exhibit intermediate adder-sizer behavior (Willis et al., 2016). Despite the recent explosion of size-homeostasis measurements, there is a lack of clarity as to the implications of these similarities and differences for mechanisms of cell-cycle control and its coupling to growth. Furthermore, despite the centrality of these concepts, how the necessity for size homeostasis limits mechanisms of cell-cycle control is not understood.

Seminal studies have revealed how cell-cycle progression is coupled to growth in several model organisms. In budding yeast, the G1/S inhibitor Whi5 is produced throughout S/G2/M and then diluted out by growth during G1 to trigger G1/S upon reaching a threshold minimum concentration (Schmoller et al., 2015). Mathematical models showed that for budding yeast-like proliferation dynamics, this "inhibitor-dilutor" G1/S regulation imparts adder behavior between birth and division (Chandler-Brown et al., 2017; Heldt et al., 2018; Soifer et al., 2016). Whi5 has functional homologs in mammals (Rb) and plants (RBR1), suggesting that an inhibitor-dilutor mechanism may regulate G1/S. In the bacterium *Escherichia coli*, the division protein FtsZ is a "master regulator" of division, with newly synthesized FtsZ accumulating at midcell proportionally with cell growth to trigger division at a total intracellular threshold level (Sekar et al., 2018; Si et al., 2019), a mechanism that recapitulates the observed adder

behavior. Similarly, active DnaA, which accumulates at the origins of replication, effects adder behavior both between consecutive G1/Ss and between consecutive divisions if it is produced proportionally with growth and triggers replication initiation (G1/S) at a threshold level per origin when it is inactivated while a fixed time or added-size increment elapses between G1/S and division (Amir, 2014; Barber et al., 2017; Ho and Amir, 2015; Logsdon et al., 2017). DnaA-mediated G1/S followed by a fixed time interval and FtsZ-mediated division may operate simultaneously in fast growth conditions, with the slower process triggering cell division (Micali et al., 2018a; Micali et al., 2018b; Si et al., 2019). DnaA and FtsZ are broadly conserved among bacteria but details of their dynamics are unknown and therefore are *a priori* expected to vary across the domain; the extent to which the requirement for size homeostasis limits their dynamics is also unknown. Master regulators also control cell cycle-checkpoint progression in eukaryotes: the broadly conserved CDK1-cyclin (Harashima et al., 2013) accumulates during growth to trigger G1/S then G2/M at successive threshold activity levels in engineered fission yeast (Coudreuse and Nurse, 2010). The CDK1-cyclin regulatory network is complex, but data indicate that it may result in a simple scaling relating active CDK1-cyclin accumulation to cell size (Keifenheim et al., 2017; Patterson et al., 2019).

In this study, we sought to develop a theoretical framework to address two major questions: how does the requirement for cell-size homeostasis limit cell-cycle regulator dynamics and mechanisms of cell-cycle checkpoint progression, and what are the implications of size-homeostasis measurements for underpinning mechanisms of cell-cycle regulation? We develop a general model of cell proliferation and use it to predict the size-homeostasis behaviors produced by a wide range of cell-cycle control mechanisms. Instances of the model focus on cells with two phases partitioned by the major eukaryotic cell-cycle checkpoints: G1/S and G2/M (assuming that G2/M and division are coincident), and on two rate-limiting mechanisms of irreversible checkpoint progression: master regulators like CDK1-cyclin or FtsZ/DnaA that accumulate to threshold activity levels, and Whi5-like inhibitor dilutors. The assumed G1 and S/G2/M phases means that the model applies to organisms with two clearly delineated phases, and not to bacteria in fast growth conditions with multiple replication forks or to fission yeast where cytokinesis between daughter cells occurs after the initiation of DNA replication. Previous models have focused on particular organisms with specific cell-cycle and growth regimes, and thus do not provide a comprehensive framework connecting proliferation dynamics to size-homeostasis measurements, or do not consider the mechanism coupling growth and cell-cycle progression and therefore lack predictive power for how genetic perturbations will affect size-homeostasis behavior. We systematically identify apparently plausible cell-cycle control scenarios that

nevertheless fail to regulate cell size and are thus impossible. We describe how growth, noise origins, cell cycle checkpoint criteria, and cell-cycle regulator dynamics differentially impact size homeostasis measurements, and how additional size homeostasis measurements may be useful to discriminate among different underlying mechanisms that cause robust deviation from adder, as observed in *A. thaliana*. Taken together, this framework and the insights it provides should be broadly useful for interpreting, motivating, and understanding the constraints governing cell-size homeostasis measurements across all organisms.

Results

A general model of cell proliferation involving two cell-cycle checkpoints

Cell-cycle regulator production and checkpoint progression

Our models consider two types of checkpoint regulators motivated by present understanding of the eukaryotic cell cycle (Fig. 1A): 1) a master regulator (e.g., CDK1-cyclin in a minimal model of fission yeast (Coudreuse and Nurse, 2010)) that accumulates from zero and triggers G1/S or G2/M progression upon reaching a intracellular threshold density within a cellular region that increases with cell size (S) as $\sim S^{\lambda_T}$ (Fig. 1A), when it is immediately degraded to zero; 2) an inhibitor dilutor (e.g. Whi5 in budding yeast (Schmoller et al., 2015)) that accumulates during one phase and is diluted out in the subsequent phase, triggering progression upon reaching a minimum threshold density with no subsequent degradation. The region of regulator accumulation grows in proportion to size if $\lambda_T = 1$ (as do most nuclei), or is independent of size if $\lambda_T = 0$ (as for genomic loci), or scales with surface area or midcell perimeter if $\lambda_T \approx 2/3$ or $1/3$, respectively (as in *Arabidopsis thaliana* apical stem cells (Willis et al., 2016)). Master regulators can accumulate through one phase, as is common for cyclins in eukaryotes, or two phases, as for CDK1-cyclin in an engineered model of fission yeast (Coudreuse and Nurse, 2010; Hochegger et al., 2008) and FtsZ/DnaA in slow-growing bacteria assuming that the same regulators operate across growth rates

with and without multiple replication forks, respectively (Si et al., 2019). Regulator production rates (dC/dt) can be cell-size dependent and may differ between phases according to

$$\frac{dC}{dt} = \kappa_{\text{phase}}\, S^{\lambda_{c,\text{phase}}}$$

where C is the number of proteins and $\lambda_{c,\text{phase}}$, κ_{phase} dictate the production rate and size dependence, respectively (Fig. 1A). The majority of proteins are thought to be maintained at constant concentrations during steady-state growth and thus are produced at a fixed rate proportional to cell size in exponentially growing cells ($\lambda_{c,\text{phase}} = 1$) (Newman et al., 2006; Padovan-Merhard et al., 2015; Schmoller and Skotheim, 2015), while Whi5 is produced independently of size through S/G2/M in budding yeast ($\lambda_{c,\text{S/G2/M}} = 0$) (Schmoller et al., 2015). In fission yeastm the activity of CDK1-cyclin may increase with a stronger size-dependence ($\lambda_{c,\text{phase}} > 1$) that results from multiple regulators with cell size-dependent levels (Keifenheim et al., 2017). The ratio of regulator production rates ($r_{\text{S/G2/M}} = \kappa_{\text{S/G2/M}}/\kappa_{\text{G1}}$) represents two extreme scenarios: either production is gene-copy number limited, meaning that the production rate doubles in S/G2/M upon gene duplication regardless of ploidy ($r_{\text{S/G2/M}} = 2$), or production is unaffected by gene-copy number ($r_{\text{S/G2/M}} = 1$) because another factor such as ribosome abundance is limiting (Heldt et al., 2018; Schmoller and Skotheim, 2015; Schmoller et al., 2015) (Fig. 1A). Proteins are assumed to be stable, consistent with measurements of key regulators, aside from targeted degradation (Hochegger et al.,

2008; Schmoller et al., 2015). For G1/S regulators, the regulator persists through cell divisions, and for simplicity we assume it is inherited in proportion to daughter cell sizes without noise.

Division and growth

In our model, cells divide into sisters with size-ratio 1:($\sigma - 1$). Thus, binary fission and asymmetric division are accounted for by $\sigma = 2$ and $\sigma \neq 2$, respectively (Fig. 1B), and at steady state cells increase their average birth size by an average factor σ over the cell cycle. The growth rate (dS/dt) can be cell size-dependent according to

$$\frac{dS}{dt} = \gamma S^{\lambda_g}.$$

While many organisms grow exponentially ($\lambda_g = 1$) (Di Talia et al., 2007; Osella et al., 2014; Soifer et al., 2016; Taheri-Araghi et al., 2015; Wang et al., 2010; Willis et al., 2016), there is some evidence of linear growth in certain regimes ($\lambda_g = 0$) (Lin and Amir, 2018). γ sets the average time scale for growth; $\ln \sigma / \gamma$ is the average cell cycle duration for exponential growth (Fig. 1C). Growth is assumed to be exponential, unless otherwise stated.

Independently regulated phases

We consider master regulators or inhibitor dilutors of G1/S or G2/M in combination with various phenomenological controls over S/G2/M or G1, respectively, including sizer, adder, or timer control, meaning that over the phase in question cells reach a critical size, add a fixed size increment, or a fixed time period elapses. Specifically, cell

size at the end of the phase ($S_{\mathrm{e,phase}}$) is determined by cell size at the beginning of the phase ($S_{\mathrm{i,phase}}$) according to

$$S_{\mathrm{e,phase}} = f_{\mathrm{phase}}\, S_{\mathrm{i,phase}} + (\sigma_{\mathrm{phase}} - f_{\mathrm{phase}})\, \mu_{\mathrm{i,phase}},$$

where f_{phase} is the mode of control ($f_{\mathrm{phase}} = 0$, 1, or σ_{phase} for sizer, adder, or timer control, respectively, and exponential growth; Methods), $\sigma_{\mathrm{phase}} > 1$ is the average fold-size increase, and $\mu_{\mathrm{i,phase}}$ is the average initial size at steady state (Fig. 1D). We refer to phases that follow this size-determination rule as independently regulated. The average fraction of the cell cycle spent in G1 at steady state (τ, which equals G1 duration $\times\ \gamma/\ln\sigma$ for exponential growth) and the mode of division (σ) determine $\sigma_{\mathrm{G1}} \approx \sigma^{\tau}$, and $\sigma_{\mathrm{S/G2/M}} \approx \sigma^{1-\tau}$ because $\sigma = \sigma_{\mathrm{G1}}\, \sigma_{\mathrm{S/G2/M}}$ (the approximations are exact for exponential growth; Methods). Average sizes at birth ($\mu_{\mathrm{i,G1}}$) and G1/S ($\mu_{\mathrm{i,S/G2/M}}$) are determined by a combination of parameters governing the average regulator dynamics ($\lambda_{c,\mathrm{phase}}$, κ_{phase}) and threshold levels or concentrations, G1 duration (τ), growth type (λ_g, γ), and division behavior (σ) (Methods).

Noise

Cell-size fluctuations emerge from noise in regulator dynamics, noise in the critical regulator density that triggers cell-cycle progression, and noise in sizer/adder/timer mechanisms. The impact of this noise on size-homeostasis behavior is encapsulated by just two parameters ($\eta_{\mathrm{G1/S}}$ and $\eta_{\mathrm{G2/M}}$; Methods) according to

200 $$\eta_{\text{checkpoint}} = \frac{\text{Noise in the transition's checkpoint mechanism}}{\text{Coefficient of variation (CV) in G1/S size}}$$

201 (Fig. 1E). For example, assuming typical values of the G1/S size CV (average/standard
202 deviation) of ~13% (Cadart et al., 2018; Taheri-Araghi et al., 2015; Willis et al., 2016), a
203 CV of ~7% in the threshold density of the G1/S checkpoint gives $\eta_{\text{G1/S}}$~0.5, while under
204 S/G2/M timer, adder, or critical size regulation, a CV of ~7% in the critical duration,
205 increment, or cell size, respectively, gives $\eta_{\text{G2/M}}$~0.5. Thus, $\eta_{\text{checkpoint}}$ is small when cell-
206 size fluctuations are primarily from noise sources other than the checkpoint (for
207 example, from fluctuations in regulator production). In later sections, motivated by
208 findings in *A. thaliana*, mammalian cells, and bacteria (Cadart et al., 2018; Ginzberg et
209 al., 2018; Nordholt et al., 2019; Willis et al., 2016), growth and production rates are
210 allowed to depend on cell birth size.
211
212 Together, this model represents a broad framework for interrogating the requirements
213 and molecular bases for cell-size homeostasis measurements. Appropriate statistics
214 were derived in terms of model parameters to estimate the combined generic effects of
215 regulator production, regulator localization, gene copy-number effects, G1 duration,
216 noise, the division mode, and the mode of control of the independently regulated phase
217 (Eqs. 1-3, Fig. 1G; Methods). To derive these slopes, we used first-order approximations
218 that were shown to reproduce size-homeostasis linear regression statistics when

deviations from the average cell size are ~10% or less (Amir, 2014; Grilli et al., 2018; Grilli et al., 2017). Major implications are outlined in the following sections.

Cell-size homeostasis requirements prohibit CDK cyclin-, FtsZ- or DnaA-like accumulators from localizing to regions that grow in proportion to the cell

It is well known that master regulators of G2/M that accumulate in proportion to cell size from zero at birth to a critical absolute level at division implement adder regulation and thus achieve size homeostasis, while production at a constant, size-independent rate fails to achieve size homeostasis in exponentially growing cells regardless of noise (Willis and Huang, 2017). In the latter case, cells multiply their birth size by a constant factor on average prior to division, so there is no negative feedback on fluctuations and cells born large become larger on average while small cells become smaller. For homeostasis of G1/S and G2/M average sizes, two criteria are that G1/S and G2/M size fluctuations must regress to their respective averages regardless of checkpoint noise, which requires that the absolute value of the slope between sizes at consecutive G1/S and G2/M transitions (Eqs. 1-3, Fig. 1G) is <1 when checkpoint noise terms ($\eta_{\text{checkpoint}}$) are set to zero (Fig. 2A). For example, the G2/M size-homeostasis requirement fails if a fixed time period T elapses between birth and division while cells grow exponentially:

$$\text{G2/M size at generation } n+1 = (\text{birth size at generation } n+1)e^{\gamma T}$$

$$= \frac{\text{G2/M size at generation } n}{\sigma} e^{\gamma T} = \text{G2/M size at generation } n$$

because at steady state $e^{\gamma T} = \sigma$. Hence, the slope between consecutive G2/M sizes is 1 and so fluctuations do not decay to the average.

We applied our model to identify other cell proliferation scenarios that fail to achieve G1/S or G2/M size homeostasis (Methods). While size homeostasis is achieved by CDK1-cyclin/FtsZ-like (G2/M) or DnaA-like (G1/S) master regulators produced from an initial level of zero in proportion to growth to trigger phase progression at a threshold level (Amir, 2014), we found that if instead progression is triggered at a critical concentration or a local threshold density in an intracellular region that scales proportionally with cell size, size homeostasis is generally lost (as λ_T increases to 1 and $\lambda_c = \lambda_{c,\mathrm{G1}} = \lambda_{c,\mathrm{S/G2/M}} = \lambda_g = 1$, $r_{\mathrm{S/G2/M}} = 1$, the slopes in Eqs. 1 and 2 (Fig. 1G) with no checkpoint noise tend to 1, regardless of other parameters). Analytical predictions were confirmed by simulations of single-cell trajectories with realistic noise levels, which produced widely varying cell sizes with characteristic long-lived deviations from the average as $\lambda_c = \lambda_{c,\mathrm{G1}} = \lambda_{c,\mathrm{S/G2/M}}$ approaches λ_g (Fig. 2Bi-iv), while G1 and S/G2/M durations and thus the ordering of G1/S and G2/M were maintained. This mechanism fails because a threshold concentration means that cell size at the checkpoint is proportional to the regulator's level, which is proportional to the added size since production is proportional to growth. Thus, cell size at the checkpoint is proportional to the added size, and ultimately cells multiply their birth size by a constant factor on

average prior to division, so there is no negative feedback on size fluctuations. For $\lambda_T = 1$, size control is lost if the size-dependence of regulator production is below that of growth ($\lambda_c < \lambda_g$), while size homeostasis is restored if $\lambda_c > \lambda_g$ (SI).

Thus, to maintain size homeostasis that is robust to the likely default mode of regulator production in proportion to biosynthetic capacity under exponential growth ($\lambda_c = \lambda_g = 1, r_{\mathrm{S/G2/M}} = 1$), the midcell bands of division-initiating FtsZ in bacteria must not increase in width proportionally as the cell grows (in which case $\lambda_T = 1$), and similarly active DnaA is prohibited from localizing to regions that grow proportionally with the cell. In eukaryotes, CDK-cyclin-like master regulators cannot trigger checkpoint progression at a local density within nuclei, since nuclei generally grow proportionally with the cell. These non-intuitive constraints emerge naturally from our model and illustrate the need for comprehensive investigation of size-homeostasis mechanisms.

DnaA accumulator-like control of G1/S likely necessitates that DnaA production or its active counterpart is in proportion to cell size

We next focused on DnaA-like G1/S two-phase master regulators that trigger checkpoint progression at a threshold absolute level ($\lambda_T = 0$) produced at a strongly size-dependent rate throughout the cell cycle ($\lambda_c = \lambda_{c,\mathrm{G1}} = \lambda_{c,\mathrm{S/G2/M}} \geq 2 + \lambda_g = 3$ for exponential growth). Our model predicts that such systems fail to robustly execute G1/S

size homeostasis (Fig. 3, S1): for S/G2/M timer or adder regulation combined with binary fission ($\sigma = 2$) and short G1 durations, fluctuations below the average G1/S size are overcompensated for in the subsequent generation (Fig. 3B, S1A,B), consistent with analytical predictions of slopes between consecutive G1/S sizes and consecutive G2/M sizes being ≤-1 (Eq. 2, Fig. 1G), so G1/S transitions frequently alternate between the beginning and end of the cell cycle (arrows in Fig. 3B). Further, if division is slightly asymmetric ($\sigma \geq 2.5$), size homeostasis of the smaller daughter is lost for short G1 durations even when $\lambda_c = 1 + \lambda_g (= 2$ for exponential growth) (Fig. 3A(vii)).

These results are intuitive: strongly size-dependent production and S/G2/M timer regulation imply that positive G1/S size fluctuations generate a large surplus of regulator at G2/M that is inherited upon division; then, the subsequent G1/S is triggered very early, with the magnitude of the G1/S size fluctuation having increased because the pace of production exceeds that of growth. Critical-size G2/M regulation eliminates the inheritance of surplus regulator, and thus restores size homeostasis (Fig. 3Aiii,vi,ix, S1C). Under strong gene copy-number effects ($r_{\mathrm{S/G2/M}} = 2$), the constraints on λ_c are more stringent (Fig. S2, S3): only $\lambda_c \approx \lambda_g (= 1$ for exponential growth) achieves robust size homeostasis for S/G2/M timer and adder regulation, while regardless of λ_c critical-size G2/M regulation invariably fails to achieve size homeostasis.

Consequently, under exponential growth and S/G2/M timer regulation, G1/S two-phase

master regulators such as DnaA robustly achieve size homeostasis only when $0 < \lambda_c < 2$, since it has been previously shown that size-independent production ($\lambda_c = 0$) cannot achieve size homeostasis. Further, the combination of G1/S two-phase master regulators and G2/M critical-size regulation is not robust to gene-copy number effects on production. These findings and those of the previous section together imply that the mode of production and mechanism of action of DnaA-like G1/S regulators are strongly constrained by the requirement of robust size homeostasis such that $\lambda_T \approx 0, \lambda_c \approx \lambda_g \approx 1$. Under these constraints and in the absence of gene copy number effects ($r_{\mathrm{S/G2/M}} = 1$), apparent adder behavior is likely to emerge between birth and division regardless of other parameters (Eq. 2, Fig. 1G). Thus, if DnaA-like G1/S control with division following replication initiation is prevalent among bacteria and if our findings hold under the extrapolation to multiple replication forks, our findings may partly explain the universality of apparent adder behavior.

Inhibitor dilutors produced at a rate that increases with the synthetic capacity of the cell are ruled out by the requirement for size control

In exponentially growing budding yeast, Whi5 executes inhibitor-dilutor control of G1/S, with Whi5 produced at a constant rate through S/G2/M while an approximately fixed time interval elapses (Schmoller et al., 2015) ($\lambda_{c,\mathrm{S/G2/M}} = 0, f_{\mathrm{S/G2/M}} = \sigma_{\mathrm{S/G2/M}}$), with G1/S being triggered at a minimal threshold concentration ($\lambda_T = 1$). Our model predicts

that in this scenario if instead the inhibitor were produced in proportion to cell size or growth ($\lambda_{c,\mathrm{S/G2/M}} = \lambda_g = 1$) or with a stronger size-dependency ($\lambda_{c,\mathrm{S/G2/M}} \geq 1$), size regulation would fail (Fig. 4Ai,ii; Eq. 3 in Fig. 1G with zero checkpoint noise ($\eta_{\mathrm{G1/S}} = \eta_{\mathrm{G2/M}} = 0$) gives a slope ≥ 1). Size control is lost as $\lambda_{c,\mathrm{S/G2/M}}$ approaches 1 because ultimately cells multiply their G1/S size ($S(T_{\mathrm{G1/S}})$) by a constant factor on average to achieve the subsequent G1/S size ($S(T_{\mathrm{G1/S}}')$):

$$S(T_{\mathrm{G1/S}}') \propto C(T_{\mathrm{G1/S}}') = C(T_{\mathrm{G2/M}})/\sigma = \frac{1}{\sigma}\left(C(T_{\mathrm{G1/S}}) + \int_{T_{\mathrm{G1/S}}}^{T_{\mathrm{G2/M}}} \kappa_{\mathrm{S/G2/M}} S\, dt\right) \propto S(T_{\mathrm{G1/S}})$$

because the inhibitor level at G1/S is $C(T_{\mathrm{G1/S}}) = S(T_{\mathrm{G1/S}}) \times$ G1/S-checkpoint threshold concentration for $\lambda_T = 1$, and $\int_{T_{\mathrm{G1/S}}}^{T_{\mathrm{G2/M}}} \kappa_{\mathrm{S/G2/M}}\, S\, dt \propto S(T_{\mathrm{G1/S}})$ owing to exponential growth. Indeed, single-cell trajectories with realistic noise levels show characteristic long-lived deviations from the average size as $\lambda_{c,\mathrm{S/G2/M}}$ approaches 1 (Fig. 4B). By contrast, for S/G2/M adder control ($f_{\mathrm{S/G2/M}} = 1$), size homeostasis is maintained as $\lambda_{c,\mathrm{S/G2/M}}$ approaches 1 and no long-lived size-deviations are observed (Fig. 4Aiii, iv), although in the limit $\lambda_{c,\mathrm{S/G2/M}} = \lambda_T > 1$ size homeostasis is lost regardless of the mode of S/G2/M control because the average G1/S size diverges (Fig. S4; Methods).

Regardless of the type of inhibitor production and the division pattern, we also found that G1/S inhibitor dilutors are incompatible with G2/M sizer mechanisms ($f_{\mathrm{S/G2/M}} = 0$) and long G1 durations ($\tau \geq 0.5$) when a threshold concentration triggers G1/S ($\lambda_T = 1$):

in this case, despite the maintenance of G2/M size via the critical-size checkpoint, G1/S sizes frequently alternate between the beginning and end of the cell cycle as τ approaches the limit for size homeostasis (Fig. 4Av, arrows in Fig. 4Bv), confirming analytical predictions of a slope of -1 between consecutive G1/S size fluctuations (Fig. 2Aii, SI). Long G1 durations can be brought about by varying parameters such as the critical G2/M size or the critical G1/S inhibitor concentration. Analogous results apply for inhibitor dilutors that trigger G2/M rather than G1/S with timer/adder/sizer control over G1 (SI).

Thus, size-homeostasis requirements prohibit the production of Whi5 or similar inhibitor dilutors in the default manner, increasing in proportion with the synthetic capacity of the cell. The combination of inhibitor dilutor and critical-size mechanisms is prohibited in cells with long G1 durations, such as plant stem cells where the G1 duration can be half the cell cycle (Dewitte et al., 2003). The model's generality and analytical tractability enabled these results (SI), which demonstrate how cell proliferation scenarios that are *a priori* biologically plausible necessarily fail to achieve size homeostasis and thus can be ruled out.

CDK cyclin-, FtsZ-, or DnaA-like accumulators maximize the rate of regression to the average cell size by minimizing growth of the regulator-localization region

The slopes in Eqs. 1-3 (Fig. 1G) reveal how the growth of regions to which regulators localize, determined by λ_T (Fig. 1A), affect the rate of regression to the average cell size. The number of generations required for fluctuations from the average cell size to decay to half their initial values equals $\ln 0.5/\ln(|\text{slope}|)$, so cell-cycle control mechanisms that generate slopes closer to zero have a more rapid decay rate (Fig. 2A). For CDK1-cyclin-/FtsZ-like G2/M two-phase master regulators, localization regions that do not expand or expand marginally with cell size ($\lambda_T \ll 1$) invariably increase the regression rate regardless of other proliferation factors (Fig. 5A; in Eq. 1 the coefficient of λ_T, $(1 - {\sigma_{\mathrm{S/G2/M}}}^{-\lambda_c} + r_{\mathrm{S/G2/M}}^{-1}\sigma^{-\lambda_c}({\sigma_{\mathrm{G1}}}^{\lambda_c} - 1))/\lambda_c$, is always positive, because necessarily $\sigma_{\mathrm{G1}} > 1$, $\sigma_{\mathrm{S/G2/M}} > 1$, and $r_{\mathrm{S/G2/M}} \geq 1$). Binary fission and default regulator production in proportion to growth ($\sigma = 2, \lambda_c = 1, r_{\mathrm{S/G2/M}} = 1$) produce a sharp decrease in the regression rate as λ_T increases from $\approx 1/2$ (Fig. 5Ai), confirmed by simulations (Fig. 5Aii). Similar results hold for G1/S DnaA-like two-phase master regulators (Fig. S5). In sum, localizing master regulators to regions that do not scale with cell size ($\lambda_T = 0$) may be a feasible strategy for maximizing the rate of regression to the average cell size regardless of other proliferation factors, while even stronger regression rates can be achieved by regulator localization regions that shrink during growth ($\lambda_T < 0$).

Size-homeostasis behaviors of budding yeast-like inhibitor dilutors respond sensitively to perturbations of S/G2/M timer regulation

In the absence of noise, G1/S Whi5-like inhibitor dilutor regulation, where the inhibitor is produced at a constant rate through S/G2/M while S/G2/M is subject to strict timer regulation, achieves overall adder behavior between consecutive G1/Ss and G2/Ms regardless of other proliferation factors, including the type of growth of the localization region when $\lambda_T > 0$ ($\lambda_{c,\mathrm{S/G2/M}} = 0$ and $f_{\mathrm{S/G2/M}} = \sigma_{\mathrm{S/G2/M}}$ produce a slope of $1/\sigma$ in Eq. 3 (Fig. 1G) with no checkpoint noise; Fig. 5B,C). This finding generalizes previous work showing apparent adder behavior among Whi5-like inhibitor dilutors controlling G1/S in specific instances pertaining to budding yeast (Chandler-Brown et al., 2017; Di Talia et al., 2007; Heldt et al., 2018; Schmoller et al., 2015; Soifer et al., 2016). Depending on λ_T and other parameters, deviations from S/G2/M timer regulation can strongly perturb the size-homeostasis behavior (Fig. 5B). Apparent sizer behavior, corresponding to the maximum rate of regression to the average cell size, is produced when $\lambda_T = (\sigma - 1)/\ln \sigma_{\mathrm{S/G2/M}} (1 - f_{\mathrm{S/G2/M}}/\sigma_{\mathrm{S/G2/M}})$ (Eq. 3, when slope=0), which corresponds to $\lambda_T \approx 1$ when S/G2/M is subject to adder regulation ($f_{\mathrm{S/G2/M}} = 1$) and approximately binary fission ($\sigma \approx 2$) regardless of G1 duration (Fig. 5D). As λ_T increases far above 1, the size homeostasis behavior converges to adder regardless of other parameters (Fig. 5B; Eq. 3).

Thus, the threshold concentration mechanism identified for G1/S-checkpoints in Whi5-budding yeast ($\lambda_T \approx 1$) is not strictly required to generate the observed adder behavior; it predicts sensitive responses to perturbations to S/G2/M timer regulation and the

production of strongly sub-adder or even apparent sizer behaviors that approximately maximize the rate of regression to the average cell size under S/G2/M adder regulation.

Noise in S/G2/M adder or timer regulation has weak effects on size-homeostasis behaviors when coupled with DnaA accumulator-like G1/S control

Eqs. 1—3 (Fig. 1G) quantify the impact of noise on apparent size homeostasis behaviors, generalizing previous work (Amir, 2014; Barber et al., 2017). For example, when production is proportional to growth in DnaA-like G1/S two-phase master regulators ($r_{\mathrm{S/G2/M}} = 1, \lambda_c = 1$ in Eq. 2), typical errors in an adder or timer S/G2/M checkpoint mechanism (measured by the CV in the added size-increment or the S/G2/M duration, respectively) generate slight and nearly identical deviations from apparent adder behavior between birth and division regardless of the division pattern (σ), the G1 duration (τ), and the growth of the regulator localization region (λ_T): assuming the CV of G1/S size is ~0.1, a ~10% G2/M checkpoint error results in a ~10% suppression of the slope between birth and division sizes (Fig. 6A, with $\eta_{\mathrm{G2/M}} = \frac{0.1}{0.1} = 1$). By contrast, the slope is strongly sensitive to G2/M checkpoint errors when the regulation is near-sizer: for $f_{\mathrm{S/G2/M}} = 0.1$, a 2% error results in a ~90% suppression, regardless of σ, τ, and λ_T (Fig. 6A, with $\eta_{\mathrm{G2/M}} = \frac{0.02}{0.1} = 0.2$).

The impact of noise can be understood qualitatively. High G2/M checkpoint noise and a non-noisy coupling between growth and regulator dynamics, which together produce high $\eta_{\mathrm{G2/M}}$, entail that cells born small contain less master regulator and therefore must produce more regulator over G1 and correspondingly grow more to achieve the threshold level for G1/S (Fig. 6B). For timer/adder regulation of S/G2/M, any compensatory growth over G1 is inherited as a positive fluctuation above the average G2/M size. Thus, the slope between birth and division is reduced by noisy G2/M checkpoint control, and this effect can be masked by other processes that contribute to G1/S size fluctuations without coupling G1/S size to birth size, such as noisy production of the G1/S regulator or noisy G1/S checkpoints. By contrast, the size homeostasis between birth and division for FtsZ- or CDK-cyclin-like G2/M regulators (Eq. 1) is unaffected by noise: noise impacts the size-homeostasis behaviors between birth and division of G1/S regulators because the production and persistence of the regulator through G2, mitosis, and division correlates birth-size fluctuations with fluctuations in birth-regulator levels; G2/M regulators are degraded or used up prior to birth, so there is no mechanism to generate such a correlation.

G1/S checkpoint noise can strongly suppress the size homeostasis behaviors of Whi5-like inhibitor dilutors

Among inhibitor dilutors, checkpoint errors have complex and potentially strong effects on size homeostasis behaviors. Noise in the threshold density for G1/S checkpoint progression ($\eta_{\mathrm{G1/S}}$) invariably suppresses the slope of birth vs. division size (Eq. 3, Fig. 1G). For a Whi5-like inhibitor with constant inhibitor production through S/G2/M where S/G2/M is subject to timer regulation, assuming the CV of G1/S size is ~0.1, a typical ~5% error in the threshold density for G1/S suppresses the slope from 1 (corresponding to apparent adder behavior) by ~30% when $\lambda_T = 1$ (Fig. 6Ci, with $\eta_{\mathrm{G1/S}} = 0.05/0.1 = 0.5$) and by ~100% when $\lambda_T = 0.5$ (Fig. 6Cii, with $\eta_{\mathrm{G1/S}} = 0.5$), regardless of the division pattern and S/G2/M duration (note that $\sigma \times$ Eq. 3 is independent of σ and τ when $\lambda_{c,\mathrm{S/G2/M}} = 0$, $f_{\mathrm{S/G2/M}} = \sigma_{\mathrm{S/G2/M}}$, and $\eta_{\mathrm{G2/M}} = 0$). When instead S/G2/M is under adder regulation, noise in the G1/S threshold density suppresses the slope by a similar degree (Fig. 6C). By contrast, the size-homeostasis response of inhibitor dilutors to noise in G2/M regulation ($\eta_{\mathrm{G2/M}}$) has a complex parameter dependence, even under constant inhibitor production and S/G2/M timer regulation (Fig. S6). For default parameters (binary fission $\sigma = 2$, S/G2/M duration $\tau = 0.5$, and $\lambda_T = 1$), G2/M checkpoint noise affects size homeostasis relatively weakly: a typical ~5% error in S/G2/M duration increases the slope of birth vs. division sizes by only ~5%, assuming a CV in G1/S size of ~0.1 (Fig. 6D, with $\eta_{\mathrm{G2/M}} = \frac{0.05}{0.1} = 0.5$).

The size homeostasis response to G1/S checkpoint noise can be understood qualitatively. Fluctuations in the G1/S checkpoint threshold density entail that a high inhibitor threshold density corresponds to small cells at G1/S, so small cells must grow more than average to dilute out the surplus inhibitor, leading to a reduction in the slope between G1/S sizes. If G1/S size fluctuations arise entirely from G1/S checkpoint noise, then the relatively small noise in inhibitor production and S/G2/M interval means that daughter cells inherit a constant amount of inhibitor at birth, and the threshold density necessary for G1/S translates into a threshold cell size, resulting in apparent sizer regulation that is inherited at the subsequent division.

Thus, among Whi5-like inhibitor dilutors, apparent adder behaviors require that size fluctuations are generated primarily by sources other than G1/S checkpoint noise, such as noise in inhibitor production and dilution. In budding yeast, deletion of *CLN3*, which leads to prolonged G1 and increased average size (Cross, 1988), or an additional copy of *WHI5* caused behavior closer to sizer for cells that were born small (Chandler-Brown et al., 2017). Our results indicate that while under S/G2/M timer regulation the inhibitor's production rate ($\kappa_{\mathrm{S/G2/M}}$) and the threshold density for G1/S progression ($\rho_{\mathrm{G1/S}}$) have no impact on size homeostasis behaviors (Eq. 3 is fully determined by $\sigma, \tau, \lambda_{c,\mathrm{S/G2/M}}, \lambda_T$ and noise terms), whereas increasing the G1/S checkpoint noise (or perturbing S/G2/M timer regulation as shown in the previous section) can induce near-sizer behavior.

Predictions for cell-cycle control mechanisms underlying intermediate sizer-adder behavior

Thus far, we have analyzed size-homeostasis statistics among systems with known or proposed mechanisms of size control. Size homeostasis measurements in the *A. thaliana* apical stem cell niche, an expanse of tissue at the plant apex that gives rise to all above-ground organs, established a linear regression slope of birth vs. division size ≈ 0.5 (Willis et al., 2016). No mechanistic model has previously been proposed to explain this intermediate behavior between sizer and adder. CDK1-cyclin species are highly conserved as major G1/S and G2/M regulators throughout eukaryotes, including *A. thaliana* (Scofield et al., 2014). Whi5 has no structural *A. thaliana* homolog, but the *A. thaliana* human retinoblastoma (RBR1) homolog plays a functional role similar to Whi5 (Harashima and Sugimoto, 2016; Turner et al., 2012), raising the possibility that *A. thaliana* G1/S is regulated by an inhibitor dilutor.

We applied our model to identify control mechanisms that could account for intermediate sizer-adder behavior. We extended our analysis to include birth-size dependent growth rates (SI) because those of *A. thaliana* stem cells were observed to correlate negatively with birth size (Willis et al., 2016), a feature that has also been observed in mammalian and bacterial cell lines (Cadart et al., 2018; Nordholt et al.,

2019). The new growth rate is $\gamma\left(1 + \alpha_g \Delta S_{\mathrm{i,G1}}\right)$, where $\Delta S_{\mathrm{i,phase}} = \frac{S_{\mathrm{i}}}{\mu_{\mathrm{i,phase}}} - 1$ is the scaled deviation from the average size at the beginning of the phase ($\mu_{\mathrm{i,phase}}$). Negative α_g enhances the growth of small cells without enhancing regulator production and thus invariably reduces the linear regression slopes between birth and division and consecutive G1/Ss among master regulators (Fig. 7A), whereas the linear regression slopes are unaffected by α_g for budding yeast-like inhibitor dilutors with constant inhibitor production and S/G2/M timer regulation regardless of σ or λ_T (SI).

In *A. thaliana* stem cells, $\alpha_g \approx -0.5$ while growth is exponential through the cell cycle ($\lambda_g = 1$), cells double their size between divisions ($\sigma = 2$), division follows shortly after G2/M (Willis et al., 2016), and the G1 duration is approximately half the cell cycle ($\sigma_{\mathrm{G1}} = 2^{0.5} = 1.4$) (Dewitte et al., 2003). Incorporating these data, we were able to immediately hypothesize two mechanisms, with distinguishing predictions for other measurable statistics.

First, a CDK1-cyclin-like G2/M two-phase master regulator produced at constant per unit size rate throughout the cell cycle ($\lambda_c = 1, r_{\mathrm{S/G2/M}} = 1$) has a linear regression slope of birth vs. division size of $1 + \alpha_g$ ($\sigma - 1$) (Fig. 7A, SI), regardless of the mode of G1/S regulation and noise levels, producing intermediate sizer-adder behavior for *A. thaliana* stem cells where $\alpha_g = -0.5, \sigma = 2$. The co-dependencies between the linear regression

slopes of birth vs. G1/S size and G1/S vs. division size are key predictions; for example, if the CVs of G1/S sizes and G2/M sizes are approximately the same (as for mammalian cells (Cadart, 2018)), a slope of approximately zero between consecutive G1/S and G2/M sizes is predicted (Fig. 7B).

Second, a budding yeast-like G1/S inhibitor dilutor produced at a constant rate through S/G2/M while S/G2/M exhibits timer regulation and a noisy G1/S threshold concentration with a typical error ~7% (thus $\eta_{\mathrm{G1/S}} \approx 0.7$, assuming a CV in G1/S size of ~0.1) gives intermediate sizer-adder behavior (Fig. 6Ci). Such a mechanism makes several distinguishing predictions: (i) a linear regression slope between birth size and G1/S size of ≈ 0.4; (ii) a linear regression slope between G1/S size and G2/M size of $\approx$ 1.2; and (iii) similar CVs of G1/S and G2/M sizes (Fig. 7C).

These examples demonstrate how our model combined with size-homeostasis statistics can generate testable hypotheses for cell cycle-control mechanisms. Other plausible mechanisms and predictions for *A. thaliana* stem cells are enumerated in Fig. S7.

Discussion

Here, we developed a general, mechanistic model of cell proliferation with two cell cycle phases, aiming to achieve a pragmatic tradeoff between the representation of cell cycle complexity and model analyzability (Fig. 1). We applied the model to determine how size homeostasis can be broken without necessarily disrupting the proper ordering of G1/S and G2/M or division across mechanisms of cell-cycle regulation under the assumption of clearly delineated G1 and S/G2/M phases. For example, our model predicts that size homeostasis would break: (1) if the width of FtsZ bands were to increase proportionally with growth to trigger division at a local threshold density (Fig. 2B); (2) more generally, if FtsZ-, CDK-cyclin-, or DnaA-like accumulators were to trigger checkpoint progression at a critical concentration while being produced in the default manner (in proportion to cellular protein content); (3) in slow-growing bacteria without multiple replication forks, if the production of DnaA activity were independent of or strongly dependent on cell size while S/G2/M was under timer control (Fig. 3B); (4) if the production of DnaA activity increased with gene-copy number while G2/M was under critical-size control (Fig. S2,S3); (5) in budding yeast, if the inhibitor dilutor Whi5 was produced in proportion to cell size rather than at a constant rate through S/G2/M (Fig. 4Bi,ii); or (6) if, while Whi5 was produced at a constant rate through S/G2/M, G2/M was under critical-size control and the G1 phase lasted for $\geq 40\%$ of the cell cycle (Fig. 4Bv-vi). These findings reveal strong and unintuitive constraints on cell-cycle regulation

551 imposed by size homeostasis requirements. They explain why certain patterns of cell
552 cycle regulation have been observed and not others, and suggest a breadth of cellular
553 designs for the loss of size homeostasis, potentially enabling experimentalists to probe
554 the physiological implications of a transient loss of size control.
555
556 We have also used our model to derive general analytical expressions connecting cell
557 cycle control mechanisms to measured size homeostasis statistics (Eqs. 1-3, Fig.1G;
558 Methods), providing a linchpin that connects genotype to size-homeostasis phenotype
559 in a broad range of scenarios. In some cases, unintuitive implications were revealed,
560 such as the potential enhancement of adder behavior by noisy regulator production
561 (Fig. 6Ai,Di,Ei), the sensitive responses of size homeostasis behaviors among Whi5-like
562 inhibitor dilutors when the mode of G2/M control or noise in the G1/S checkpoint are
563 perturbed (Fig. 5B, 6D), and the size-homeostasis optimizing strategy to minimize the
564 growth of regulator localization regions among FtsZ-, CDK-cyclin-, or DnaA-like
565 accumulators (Fig. 5A).
566
567 We have inevitably approximated or omitted certain details of cell proliferation;
568 nevertheless, our analytical derivations are a powerful basis for generating and testing
569 hypotheses across a range of scenarios and can be adapted to account for additional
570 features of proliferation (SI). To exemplify this power, we enumerated mechanisms that

account for the intermediate sizer-adder behavior between birth and division observed in *A. thaliana* apical stem cells, with distinguishing predictions for other size-homeostasis statistics (Fig. 7). One plausible mechanism assumes CDK1-cyclin behaves as a master regulator triggering G2/M at a threshold level and is produced proportionally with cell size rather than growth rate throughout the cell cycle, thus implying that regulator production scales with bulk synthetic capacity of the cell (which presumably scales with size) rather than being directly coupled to growth. Then, if the CVs in cell size at G1/S and G2/M are similar, apparent near-sizer behavior over S/G2/M, corresponding to a zero correlation between G1/S size and G2/M size, is predicted (Fig. 7B). These predictions can be readily tested by quantitative time-lapse imaging of *A. thaliana* apical stem cells in strains containing extant G1/S and membrane reporters (Jones et al., 2017; Willis et al., 2016).

Our model also allows us to address important open questions regarding size control. Why is adder behavior ubiquitous? The cellular machinery for the initiation of DNA replication and division must be coupled to growth to ensure both that division takes place after the termination of DNA replication and an efficient balance of cellular components is maintained, the latter necessitating the maintenance of an optimal average cell size. Our results demonstrate that achieving this maintenance is a non-trivial task, and thus suggest that adder behavior may result from conserved

mechanisms tuned within a set of physiological limits to be maximally robust to commonly or necessarily experienced fluctuations in proliferation that could otherwise cause catastrophic loss of size control. For example, threshold concentration mechanisms may be selected against among FtsZ-, CDK1-cyclin-, and DnaA-like accumulators because such mechanisms cannot withstand the default mode of regulator production in proportion to biosynthetic capacity, which may be brought about commonly by mutations or certain physiological conditions that require events triggered by the regulator to occur only when cellular machineries are sufficiently plentiful. In bacteria, where DnaA-like accumulators operate between consecutive G1/Ss, for size homeostasis to be maximally robust to fluctuations in the growth rate compared with the S/G2/M duration ($1 - \tau$), division-plane positioning, and gene-copy number effects on the production of DnaA, DnaA must be produced approximately in proportion to biosynthetic capacity (Fig. 3A, S1-S3). Both of the above mechanisms result in approximate adder or apparent adder behavior between birth and division that is observed largely regardless of noise in the average cellular behaviors (Eqs. 1,2, Fig. 1G; Fig. 6A).

In general, our findings exemplify how the model combined with quantitative time-lapse measurements of cell size dynamics and cell cycle reporters across species, mutants, and conditions should both help to establish the mechanisms of cell cycle

611 regulation, and further illuminate their necessity for size control. The intimate
612 connections between maintaining a specific average cell size and other cellular
613 processes should also be an important factor in probing the response of cells to non-
614 steady-state conditions and to the future design of artificial cells.

Acknowledgements

The authors thank members of the Huang Laboratory and Clotilde Cadart, Po-Yi Ho, Benjamin Knapp, and Fred Chang for helpful discussions. This work was supported by the Allen Discovery Center at Stanford on Systems Modeling of Infection (to K.C.H.) and the Gatsby Charitable Foundation under Grant GAT3395/PR4 (to H.J.). K.C.H. is a Chan Zuckerberg Biohub Investigator. This work was also supported in part by the National Science Foundation under Grant PHYS-1066293 (to K.C.H.) and the hospitality of the Aspen Center for Physics.

Author Contributions

Conceptualization, L.W., H.J., and K.C.H.; Methodology, L.W. and K.C.H.; Formal analysis, L.W.; Writing-Original draft, L.W. and K.C.H.; Writing-Review and editing, L.W., H.J., and K.C.H.; Funding acquisition, L.W., H.J., and K.C.H.

Declarations of Interests

The authors declare no competing interests.

Figure Legends

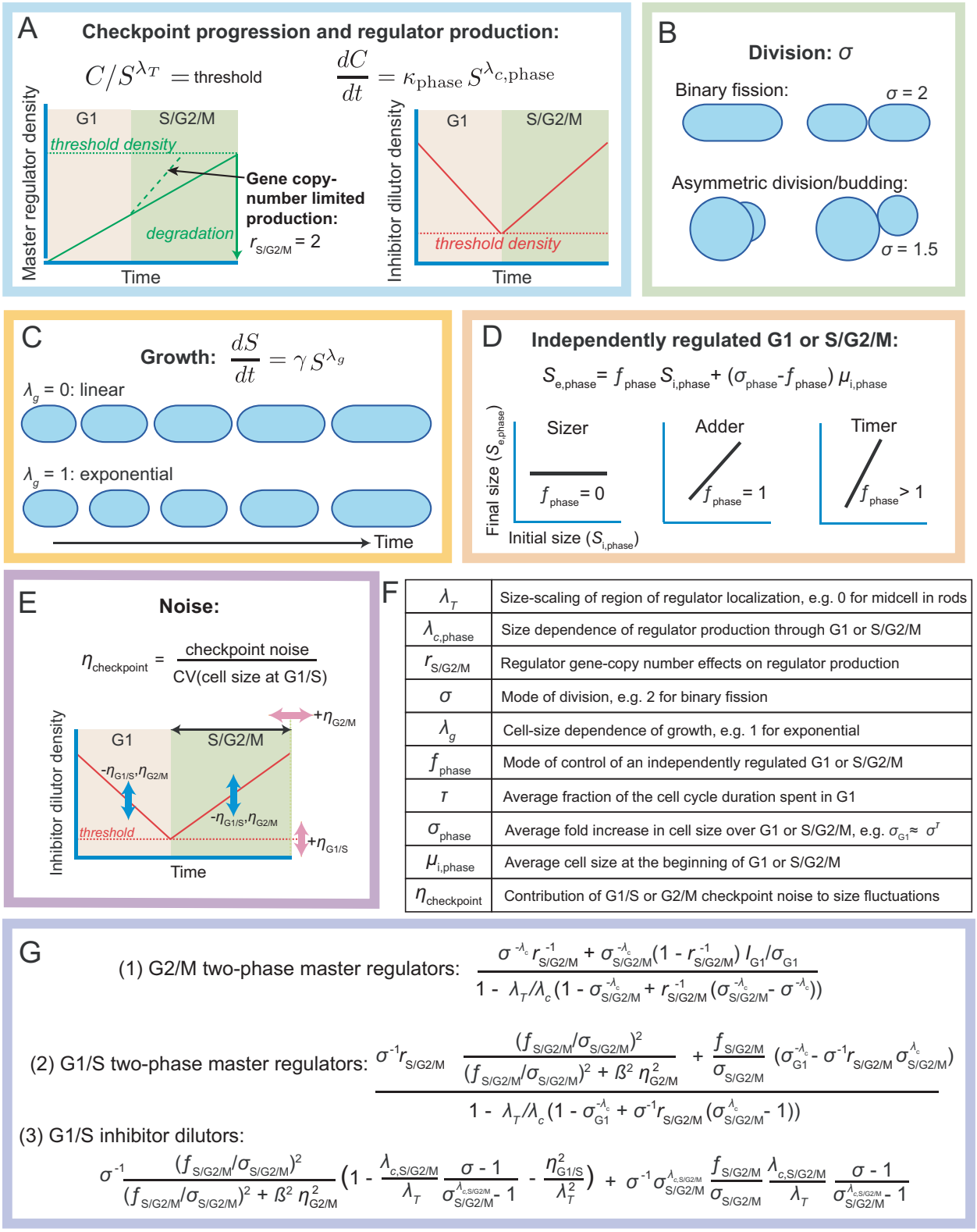

F

λ_T	Size-scaling of region of regulator localization, e.g. 0 for midcell in rods
$\lambda_{c,\text{phase}}$	Size dependence of regulator production through G1 or S/G2/M
$r_{S/G2/M}$	Regulator gene-copy number effects on regulator production
σ	Mode of division, e.g. 2 for binary fission
λ_g	Cell-size dependence of growth, e.g. 1 for exponential
f_{phase}	Mode of control of an independently regulated G1 or S/G2/M
τ	Average fraction of the cell cycle duration spent in G1
σ_{phase}	Average fold increase in cell size over G1 or S/G2/M, e.g. $\sigma_{G1} \approx \sigma^{\tau}$
$\mu_{i,\text{phase}}$	Average cell size at the beginning of G1 or S/G2/M
$\eta_{\text{checkpoint}}$	Contribution of G1/S or G2/M checkpoint noise to size fluctuations

G

(1) G2/M two-phase master regulators:

$$\frac{\sigma^{-\lambda_c} r_{S/G2/M}^{-1} + \sigma_{S/G2/M}^{-\lambda_c}(1 - r_{S/G2/M}^{-1})\, I_{G1}/\sigma_{G1}}{1 - \lambda_T/\lambda_c (1 - \sigma_{S/G2/M}^{-\lambda_c} + r_{S/G2/M}^{-1}(\sigma_{S/G2/M}^{-\lambda_c} - \sigma^{-\lambda_c}))}$$

(2) G1/S two-phase master regulators:

$$\frac{\sigma^{-1} r_{S/G2/M} \dfrac{(f_{S/G2/M}/\sigma_{S/G2/M})^2}{(f_{S/G2/M}/\sigma_{S/G2/M})^2 + \beta^2 \eta_{G2/M}^2} + \dfrac{f_{S/G2/M}}{\sigma_{S/G2/M}} (\sigma_{G1}^{-\lambda_c} - \sigma^{-1} r_{S/G2/M} \sigma_{S/G2/M}^{\lambda_c})}{1 - \lambda_T/\lambda_c (1 - \sigma_{G1}^{-\lambda_c} + \sigma^{-1} r_{S/G2/M} (\sigma_{S/G2/M}^{\lambda_c} - 1))}$$

(3) G1/S inhibitor dilutors:

$$\sigma^{-1} \frac{(f_{S/G2/M}/\sigma_{S/G2/M})^2}{(f_{S/G2/M}/\sigma_{S/G2/M})^2 + \beta^2 \eta_{G2/M}^2} \left(1 - \frac{\lambda_{c,S/G2/M}}{\lambda_T} \frac{\sigma - 1}{\sigma_{S/G2/M}^{\lambda_{c,S/G2/M}} - 1} - \frac{\eta_{G1/S}^2}{\lambda_T^2}\right) + \sigma^{-1} \sigma_{S/G2/M}^{\lambda_{c,S/G2/M}} \frac{f_{S/G2/M}}{\sigma_{S/G2/M}} \frac{\lambda_{c,S/G2/M}}{\lambda_T} \frac{\sigma - 1}{\sigma_{S/G2/M}^{\lambda_{c,S/G2/M}} - 1}$$

Figure 1: A general model of cell proliferation with two cell-cycle checkpoints.

(A) Checkpoint progression is triggered at a threshold regulator density in a region that scales with cell size (S) as S^{λ_T}: $\lambda_T = 1$ means that the region scales proportionally with size (as do most nuclei) while $\lambda_T = 0$ means that the region is size-independent (as for FtsZ midcell localization in rod-shaped bacteria). The dependence of cell-cycle regulator production rate $\left(\frac{dC}{dt}\right)$ on S is dictated by $\lambda_{c,\mathrm{phase}}$, with the phase corresponding to either G1 or S/G2/M. $\lambda_{c,\mathrm{phase}} = 1$ corresponds to size-proportional production. Master regulators (left) are produced throughout one or both phases at a rate that can increase with gene-copy number (corresponding to $r_{\mathrm{S/G2/M}} = \kappa_{\mathrm{S/G2/M}}/\kappa_{\mathrm{G1}} = 2$) to trigger G1/S or G2/M, then are degraded. Inhibitor dilutors (right) are produced throughout one phase only ($\kappa_{\mathrm{G1}} = 0$) and then diluted out in the next phase. G1/S or G2/M are triggered when the regulator reaches a threshold density in a region that scales with cell size as $\sim S^{\lambda_T}$.

(B) Cell division can occur through binary fission ($\sigma = 2$) or asymmetrically ($\sigma < 2$ or $\sigma > 2$).

(C) Cell growth is exponential, linear, or intermediate ($\lambda_g = 1, 0$, or otherwise, respectively). Unless otherwise stated, growth is assumed to be exponential.

(D) Cell cycle regulators can operate in combination with an independently regulated G1 or S/G2/M phase, meaning that the size at the end of the phase

($S_{\mathrm{e,phase}}$) depends only on the size at the beginning of the phase ($S_{\mathrm{i,phase}}$) and not on prior sizes, with the mode of regulation dictated by f_{phase}: $f_{\mathrm{phase}} = 0, 1$ or σ_{phase} for critical size (sizer), adder, or timer regulation, respectively (Methods). σ_{phase} is the steady-state average fold increase in cell size over the phase; $\sigma_{\mathrm{G1}} \approx \sigma^{\tau}$, where τ is the fraction of the cell cycle taken up by G1, and $\sigma_{\mathrm{S/G2/M}} \approx \sigma^{1-\tau}$. The average initial size $\mu_{\mathrm{i,phase}}$ can be expressed in terms of other model parameters (Methods).

(E) Cell-size fluctuations are due to noise in regulator dynamics and cell-cycle checkpoints. Noise effects are summarized by $\eta_{\mathrm{G1/S}}$ and $\eta_{\mathrm{G2/M}}$, corresponding to the noise in the G1/S and G2/M checkpoint criteria, respectively, divided by the coefficient of variation (CV) in G1/S size. For example, the G2/M checkpoint noise of S/G2/M timer control equals the CV of the fixed time period between G1/S and G2/M (horizontal pink arrow); for G1/S inhibitor dilutors, the G1/S checkpoint noise corresponds to the CV in the threshold density for checkpoint progression (vertical pink arrow). Noise sources that increase CV(cell size at G1/S) without affecting the noise checkpoint, for example noise in the production or dilution of the inhibitor (blue arrows), reduce $\eta_{\mathrm{G1/S}}$ and $\eta_{\mathrm{G2/M}}$.

(F) Definitions of key parameters determining size-homeostasis behaviors.

(G) The linear regression slopes between birth sizes in two consecutive generations for CDK1-cyclin/FtsZ-like G2/M two-phase master regulators (Eq. 1), DnaA-like

G1/S two-phase master regulators (Eq. 2), and Whi5-like G1/S inhibitor dilutors (Eq. 3), assuming exponential growth ($\lambda_g = 1$) and a persistent size-dependent production through both phases ($\lambda_c = \lambda_{c,\mathrm{G1}} = \lambda_{c,\mathrm{S/G2/M}}$) for two-phase master regulators. The parameter $\beta = 1 - \frac{f_{\mathrm{S/G2/M}}}{\sigma_{\mathrm{S/G2/M}}}(1 - \ln f_{\mathrm{S/G2/M}})$. Derivations and expressions for further size-homeostasis statistics are in Methods and SI.

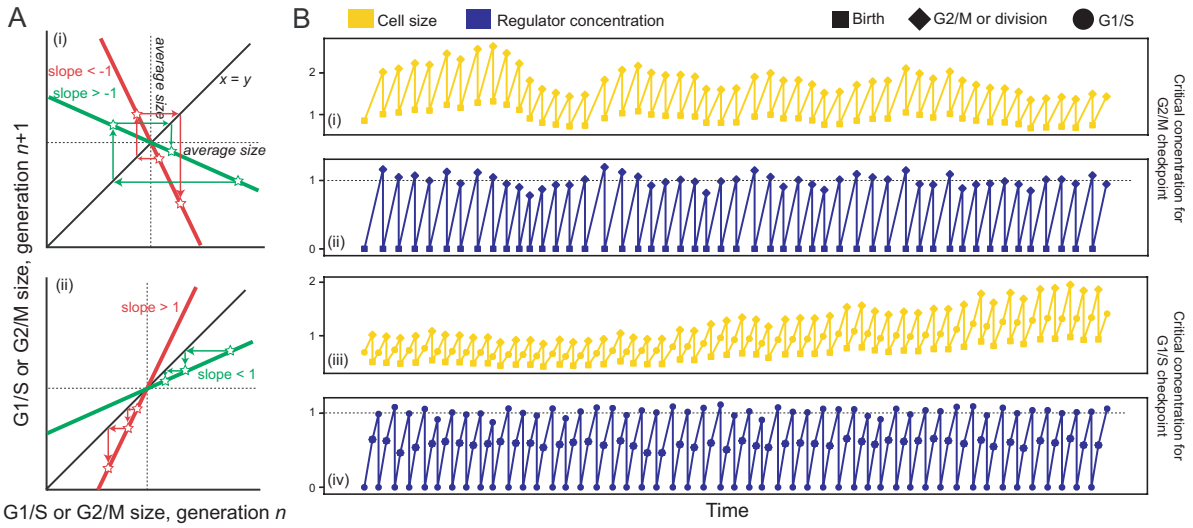

Figure 2: Size-homeostasis requirements prohibit critical concentration checkpoint mechanisms among CDK-cyclin, FtsZ- or DnaA-like regulators when production is proportional to growth.

(A) For cells to achieve size homeostasis, the linearized relationship between cell sizes at G1/S or G2/M in consecutive cell cycles must have a slope between -1 and 1 (green trajectories, Methods), otherwise size fluctuations diverge from the average (red trajectories).

(B) Simulations of single-cell lineages with realistic noise levels confirm analytical results, that regulators produced in proportion to growth ($\lambda_c = \lambda_{c,\mathrm{G1}} = \lambda_{c,\mathrm{S/G2/M}} = \lambda_g$) from an initial level of zero to trigger checkpoint progression at a noisy threshold concentration (dotted lines in (ii) & (iv)) fail in size homeostasis. (i,ii) a G2/M master regulator undergoing binary fission ($\sigma = 2$) with size-dependent production $\lambda_c = \lambda_{c,\mathrm{G1}} = \lambda_{c,\mathrm{S/G2/M}} = 1.05$ similar to the size-

dependence of growth $\lambda_g = 1$. (iii,iv) a G1/S two-phase master regulator with $\lambda_c = \lambda_{c,\mathrm{G1}} = \lambda_{c,\mathrm{S/G2/M}} = 1.005$ approaching $\lambda_g = 1$, and $\sigma = 2, \tau = 0.5$. Cell sizes fluctuate dramatically as λ_c approaches λ_g, and size homeostasis is lost in the limit $\lambda_c = \lambda_g$.

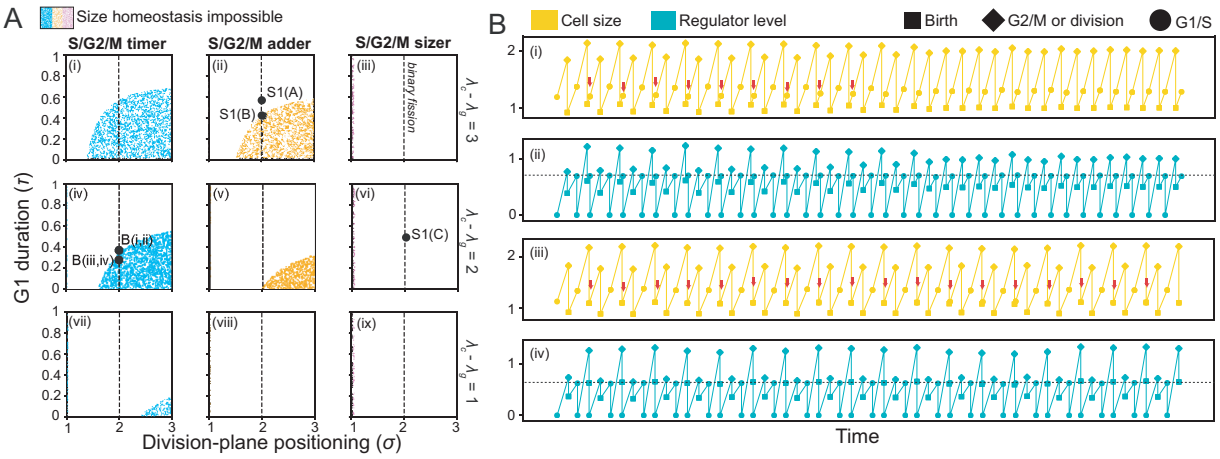

Figure 3: DnaA accumulator-like control of G1/S likely necessitates that DnaA production is approximately in proportion to cell size.

(A) G1/S DnaA-like two-phase master regulators that trigger phase progression at a threshold level ($\lambda_T = 0$) with no gene copy number effects ($r_{\mathrm{S/G2/M}} = 1$) lose size homeostasis over a range of division-plane positions (σ; x-axis) and G1 durations (τ; y-axis), according to whether the absolute value of the slope of G1/S size in generation n vs. generation n+1 is >0.95, as shown by colored regions. Regulators with strongly size-dependent production rates ($\lambda_c = \lambda_{c,\mathrm{G1}} = \lambda_{c,\mathrm{S/G2/M}} > \lambda_g + 1$ (= 2 for exponential growth); rows) tend to lose size homeostasis particularly when S/G2/M is under timer regulation (left column). Black circles correspond to single-cell lineages simulated in (B).

(B) Simulations of G1/S two-phase master regulators corresponding to black circles in (Aiv) demonstrate that G1/S sizes and consequently G2/M sizes

overshoot then undershoot the averages. The oscillatory dynamics are transient when the G1 duration (τ) is close to the limit ($\tau = 0.37$, i,ii), then persistent as τ reaches the limit ($\tau = 0.3$, iii,iv). Red arrows point to cell cycles where G1/S occurred near the end of the cell cycle; in the following cell cycle, G1/S tends to occur early.

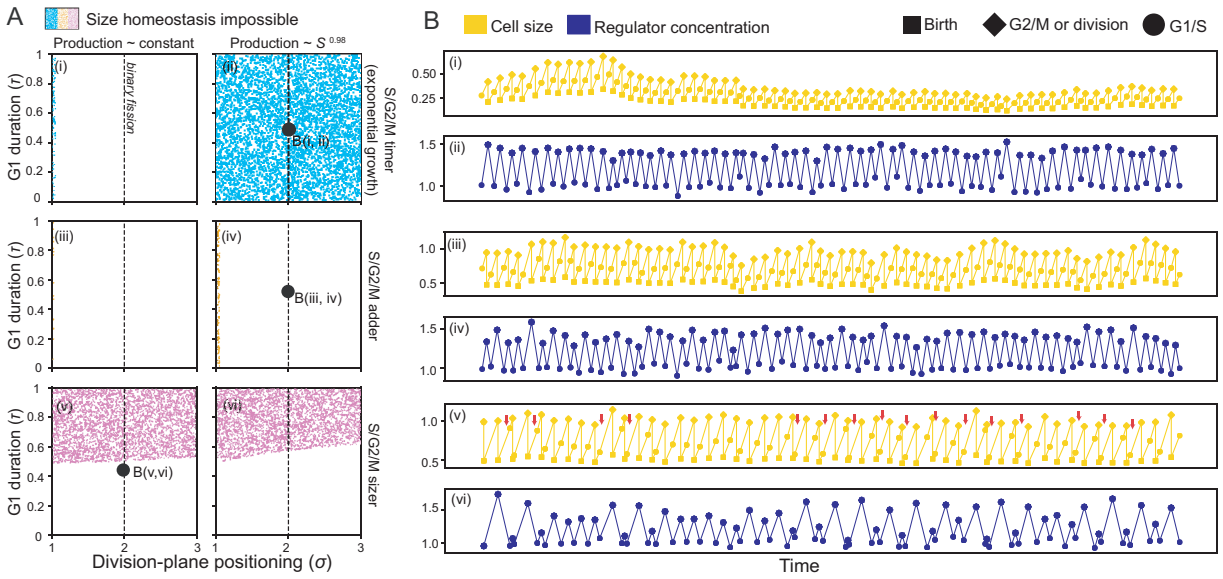

Figure 4: Inhibitor dilutors produced at a rate increasing with the synthetic capacity of the cell are ruled out by the requirement for size control.

(A) Colored regions indicate where G1/S size homeostasis is nearly lost (absolute value of slope between consecutive G1/S sizes < 0.95; SI) for a range of division-plane positions (σ; x-axis), G1 durations (τ; y-axis), different modes of S/G2/M regulation ($f_{S/G2/M}$; rows), when a minimum threshold concentration triggers G1/S progression ($\lambda_T = 1$), and inhibitor production is constant ($\lambda_{c,S/G2/M} = 0$; left) or nearly proportional to cell size ($\lambda_{c,S/G2/M} = 0.98$; right). (i, ii) If S/G2/M is under timer regulation, size homeostasis is maintained if inhibitor production is constant, as for Whi5 in budding yeast, but is lost if inhibitor production is proportional to cell size. (iii,iv) S/G2/M

adder regulation generally maintains size homeostasis. (v,vi) Regardless of growth and production patterns, for $\lambda_T = 1$ G1/S inhibitor dilutors are incompatible with the combination of G2/M sizer regulation ($f_{\mathrm{S/G2/M}} = 0$) and long G1 durations ($\tau \geq 0.5$). Black circles correspond to single-cell lineages simulated in (B).

(B) Simulations of G1/S inhibitor dilutors corresponding to the black circles in (A) confirm analytical results. (i,ii) Cell size and inhibitor concentration control are nearly lost for a budding yeast-like inhibitor dilutor ($\sigma = 2, \tau = 0.5, \lambda_g = 1$, and S/G2/M timer regulation) when the inhibitor's production grows nearly in proportion to cell size ($\lambda_{c,\mathrm{S/G2/M}} = 0.98$) rather than at a constant rate. (iii, iv) Switching to S/G2/M adder regulation restores size homeostasis. (v,vi) G2/M critical size control causes loss of G1/S size homeostasis if the G1 duration is long ($\sigma = 2, \tau = 0.45$). Red arrows point to cell cycles where G1/S occurred near the end of the cell cycle; in the following cell cycle, G1/S tends to occur early.

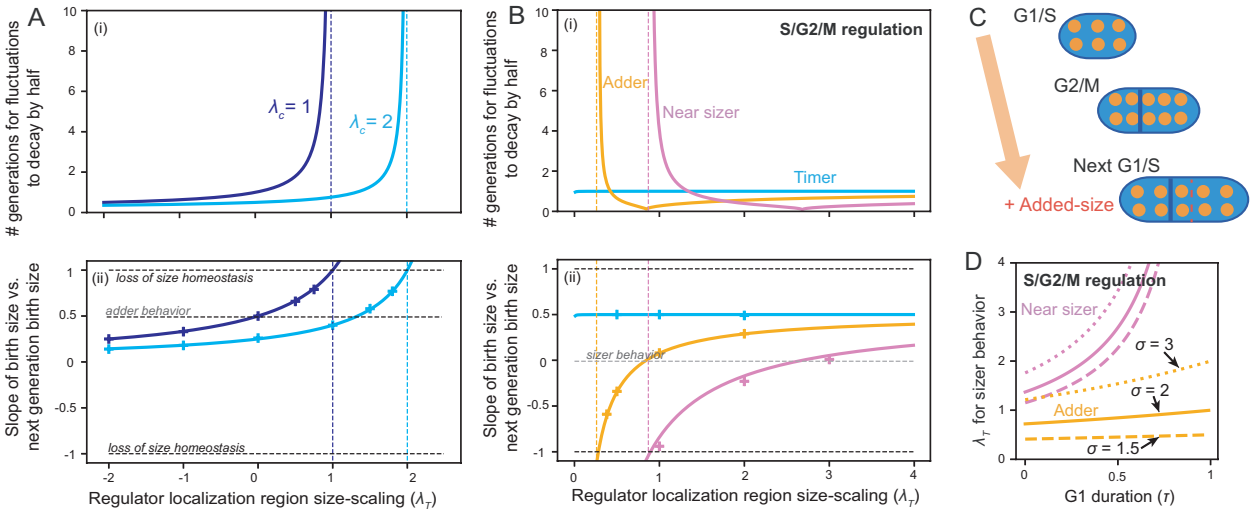

Figure 5: Size homeostasis behaviors vary with the type of growth of the regulator-localization region.

(A)(i) For FtsZ- and CDK-cyclin-like accumulators that trigger G2/M, the number of generations required for size fluctuations to decay to half their initial values (half-life) decreases as the size-dependence of the regulator localization region (λ_T) decreases toward and below 0, $\lambda_T = 0$ being brought about by, for example, the accumulation of the regulator at mid-cell in rod-shaped cells. (ii) Correspondingly, the slope of birth size vs. birth size in the next generation tends to 0. Plots are for no gene-copy number effect ($r_{\mathrm{S/G2/M}} = 1$, thus τ and S/G2/M regulation have no impact on size homeostasis) and binary fission ($\sigma = 2$). For default production in proportion to exponential growth ($\lambda_c = \lambda_g$), the half-life blows up when λ_T exceeds $\approx \frac{1}{2}$, and reaches the limits for size homeostasis at the

vertical dashed lines. Cross-bars represent exact simulations that agree with analytical results (Methods).

(B) Whi5-like G1/S inhibitor dilutors with constant inhibitor production through S/G2/M. Deviations from S/G2/M timer regulation to adder ($f_{\mathrm{S/G2/M}} = 1$;orange) and near-sizer ($f_{\mathrm{S/G2/M}} = 0.1$; pink) reveal minima in the half-lives of cell size fluctuations and thus maxima in the regression rates to the average cell size (i), corresponding to a slope of 0 between consecutive birth sizes and thus apparent sizer behavior in the case of low checkpoint noise, $\sigma = 2$, $\tau = 0.5$ (ii). Cross-bars represent exact simulations.

(C) Addition of a constant amount of inhibitor (orange spots) over S/G2/M achieves adder size homeostasis between consecutive G1/Ss, because added size scales with amount of inhibitor produced regardless of the size-scaling of the inhibitor's localization region.

(D) For inhibitor dilutors as in (B), apparent sizer behavior (with a slope of 0 between consecutive birth sizes) is achieved when $\lambda_T = (\sigma - 1)/\ln \sigma_{\mathrm{S/G2/M}}\,(1 - f_{\mathrm{S/G2/M}}/\sigma_{\mathrm{S/G2/M}})$ where $\sigma_{\mathrm{S/G2/M}} = \sigma^{1-\tau}$. This value is consistently close to 1 when S/G2/M is subject to adder regulation (orange; $f_{\mathrm{S/G2/M}} = 1$) and $\sigma \approx 2$ regardless of G1 duration (τ).

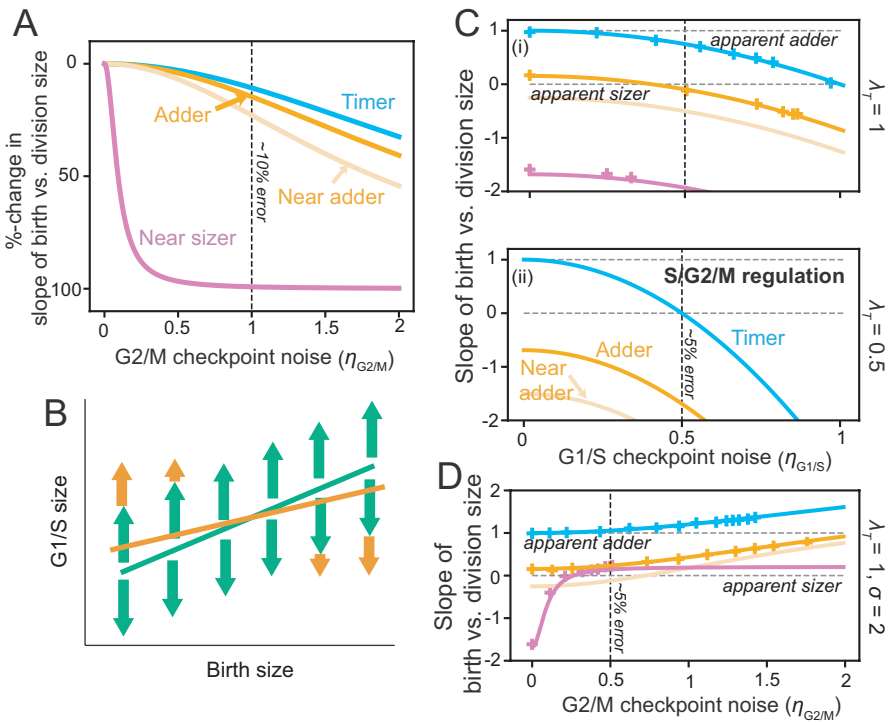

Figure 6: The quantitative and qualitative effects of noisy cell-cycle checkpoints on size homeostasis measurements.

(A) For DnaA-like G1/S two-phase master regulators with production proportional to growth ($r_{S/G2/M} = 1, \lambda_c = 1$), regardless of the values of λ_T and σ, the %-change in the slope of birth vs. division size is relatively weak and nearly identical for S/G2/M timer and S/G2/M adder regulation as the G2/M checkpoint noise increases to $\eta_{G2/M}$~1 (corresponding to a typical error of ~10% in the S/G2/M timer or adder mechanism assuming a CV in G1/S size of 0.1). Slopes are sensitively affected by G2/M checkpoint noise as G2/M sizer regulation is approached (pink vs. blue/orange). Timer, adder, near-adder, or near-sizer correspond to $f_{S/G2/M} = \sigma_{S/G2/M}$, 1, 0.8, or 0.1, respectively.

(B) Among G1/S two-phase master regulators, relatively high noise in the G2/M checkpoint mechanism results in small or large cells at birth with low or high regulator levels, respectively. Small cells then grow more and thus produce more regulator to achieve the surplus regulator level for G1/S progression (orange arrows). Noise sources that impact the regulator's production and G1/S checkpoint mechanism are uncoupled from initial birth size, and thus do not affect the size homeostasis behavior between birth and G1/S (green arrows).

(C) Whi5-like inhibitors with constant production through S/G2/M combined with S/G2/M timer regulation produce birth size vs. division size slopes that may depend strongly on G1/S checkpoint noise ($\eta_{\mathrm{G1/S}}$), while they are unaffected by σ or τ. Assuming zero G2/M checkpoint noise and a CV of G1/S size of ~0.1, typical ~5% errors in the G1/S threshold density suppress the slopes by ~30% or ~100% when $\lambda_T = 1$ (i) or $\lambda_T = 0.5$ (ii), thus producing apparent sub-adder or near sizer behavior. For S/G2/M adder, near adder, or near sizer regulation ($f_{\mathrm{S/G2/M}} = 1$, 0.8, or 0.1, respectively), the slopes are all strongly suppressed by typical ~5% errors in the G1/S checkpoint. Cross-bars represent simulations with realistic size fluctuations.

(D) Under binary fission, $\tau = 0.5$, and $\lambda_T = 1$, inhibitor dilutors with constant production through S/G2/M are relatively weakly affected by G2/M checkpoint noise ($\eta_{\mathrm{G2/M}}$) for S/G2/M timer, adder, or near adder regulation ($f_{\mathrm{S/G2/M}} = 2^{0.5}, 1,$

808 or 0.8). Typical ~5% errors increase birth size vs. division size slopes by ~5%,

809 assuming a CV in G1/S size of ~0.1 and $\eta_{\mathrm{G1/S}} = 0$. The response is much stronger

810 for S/G2/M near-sizer regulation ($f_{\mathrm{S/G2/M}} = 0.1$).

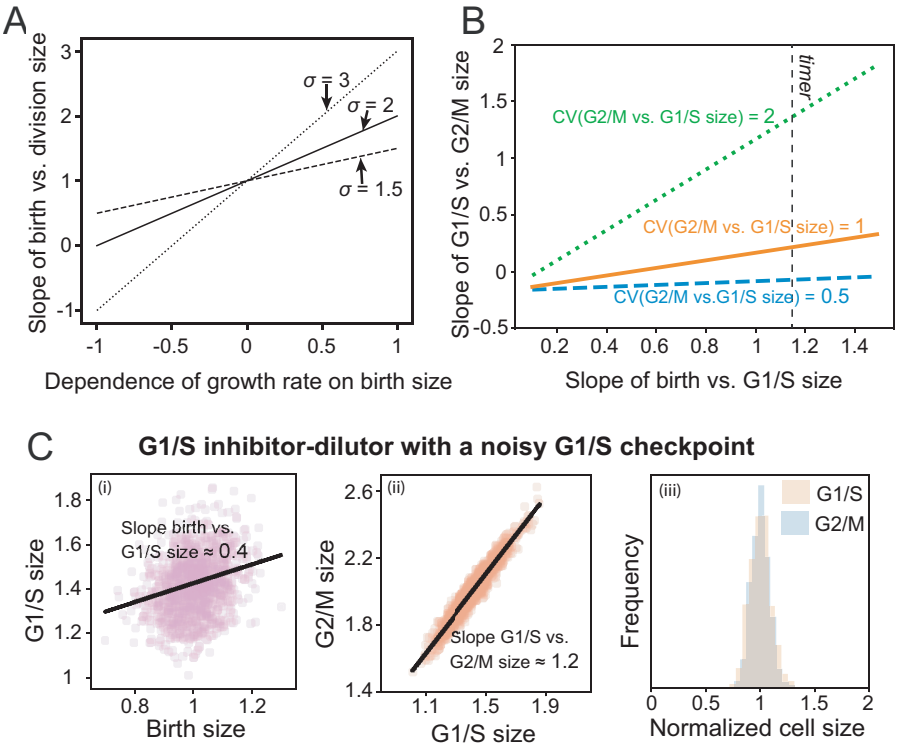

811

812 **Figure 7: Predictions for cell-cycle control mechanisms underlying intermediate sizer-**

813 **adder behavior.**

814 (A) The linear regression slope of birth vs. division size depends on the link between

815 birth size and growth rate (α_g, x-axis; negative α_g means small cells grow faster).

816 In exponentially growing cells with a master regulator produced in proportion to

817 cellular synthetic capacity with no birth-size dependence ($\lambda_c = 1, r_{\mathrm{S/G2/M}} = 1$), the

818 linear regression slope of birth vs. division size is $1 + \alpha_g\ (\sigma - 1)$, so $\alpha_g \neq 0$ causes

819 deviations from adder behavior. In *A. thaliana* stem cells, measurements show $\alpha_g \approx$

820 $-0.5, \sigma = 2$, giving a slope of ≈ 0.5.

821 (B) From (A), CDK1-cyclin-like G2/M two-phase master regulators with $\lambda_c =$

822 $1, r_{\mathrm{S/G2/M}} = 1$ give intermediate sizer-adder behavior, as observed in *A. thaliana*

stem cells. This mechanism predicts a relationship between the slope of birth vs. G1/S size (x-axis), the slope of G1/S vs. division size (y-axis), and the ratio of CV(cell size at G2/M):CV(cell size at G1/S). If CV(cell size at G2/M) ≤ CV(cell size at G1/S), the slope of G1/S vs. division size is close to 0 regardless of the size homeostasis behavior over G1.

(C) A budding yeast-like inhibitor dilutor produced at a constant rate through S/G2/M while S/G2/M is under timer regulation produces intermediate size-adder behavior if the G1/S checkpoint is relatively noisy with a typical error of ~7%. Predictions are (i) a linear regression slope between birth vs. G1/S size of ≈ 0.4; (ii) a slope between G1/S vs. G2/M size of ≈ 1.2; (iii) similar CV(cell size at G2/M) ≈ CV(cell size at G1/S).

Supplemental Figures

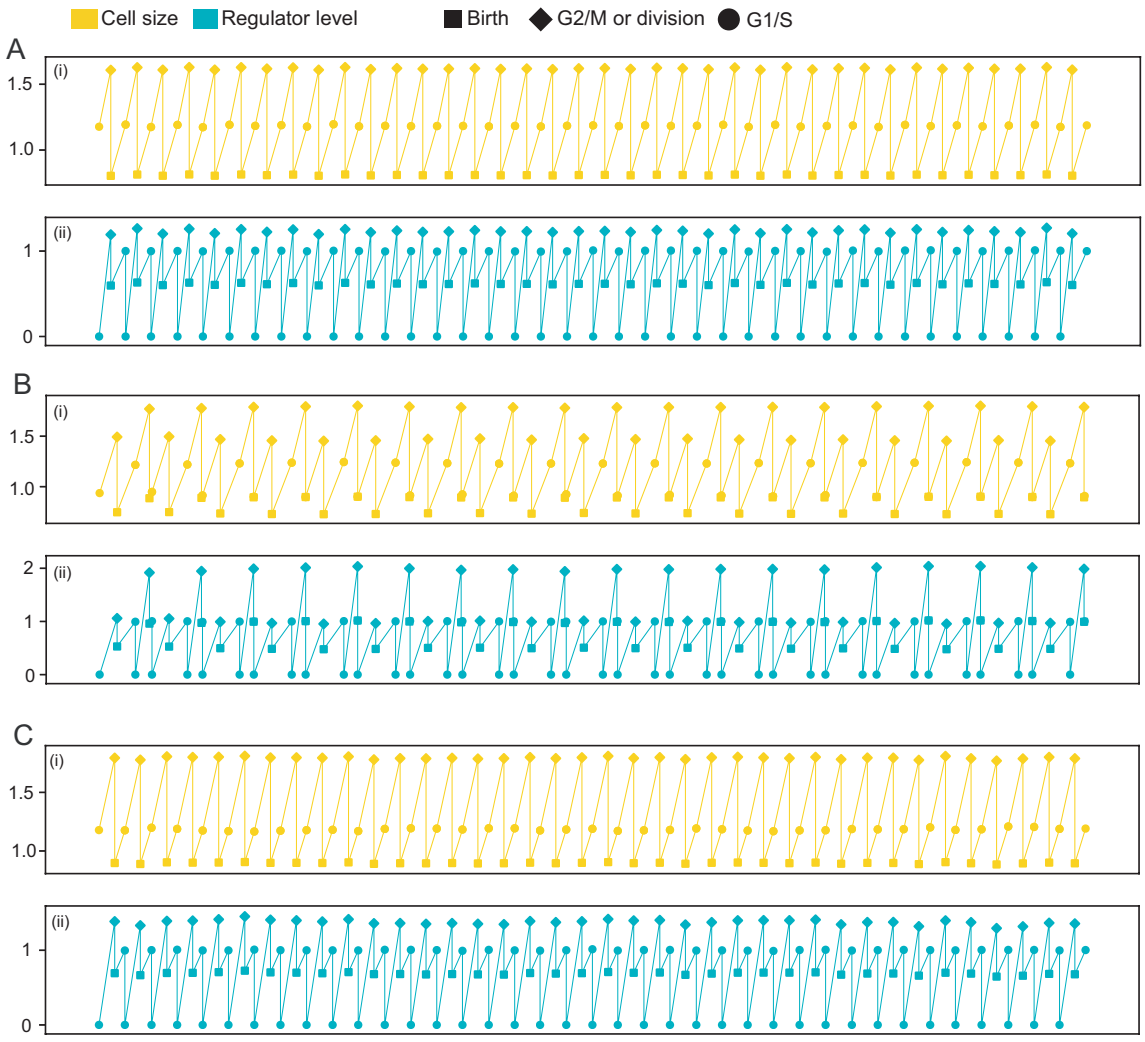

Figure S1: Simulations support analytical predictions of a loss of cell-size homeostasis. Simulations of single-cell trajectories from Fig. 3A. Cells are exponentially growing with G1/S under DnaA-like two-phase master regulator control triggering checkpoint progression at a threshold absolute level ($\lambda_T = 0$).

(A) In simulations corresponding to Fig. 3A(ii) of cells under a strongly size-dependent production rate ($\lambda_c = \lambda_{c,\mathrm{G1}} = \lambda_{c,\mathrm{S/G2/M}} = 4$), S/G2/M adder

842 regulation combined with binary fission ($\sigma = 2$) exhibits size homeostasis
843 when $\tau = 0.55$.
844 (B) However, size homeostasis is lost when $\tau = 0.41$, with other parameters as in
845 (A); then, G1/S transitions alternate between the beginning (when they are
846 coincident with birth) and the end of the cell cycle, consistent with analytical
847 predictions of a slope between consecutive G1/S sizes ≤-1.
848 (C) In simulations corresponding to Fig. 3A(vi), critical-size G2/M regulation
849 maintains size homeostasis regardless of the size dependence of the
850 production rate. Here, $\lambda_c = 3$, $\sigma = 2$, and $\tau = 0.5$.

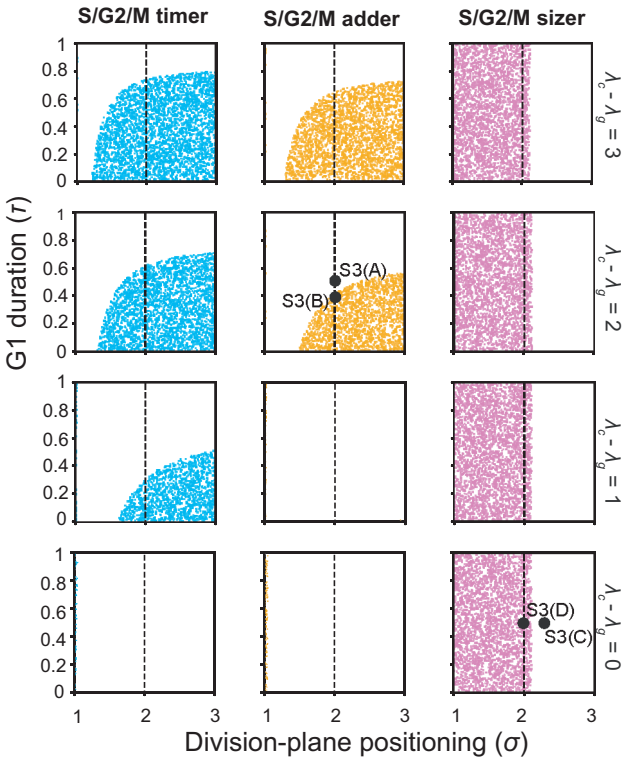

Figure S2: The loss of size homeostasis for DnaA-like G1/S two-phase master regulators with gene copy-number production effects.

Analytical results for whether G1/S DnaA-like two-phase master regulators that trigger phase progression at a threshold level ($\lambda_T = 0$) with a gene copy-number dependent production rate ($r_{\mathrm{S/G2/M}} = 2$) lose size control (colored regions) over a range of division-plane positions (σ; x-axis) and G1 durations (τ; y-axis), according to whether the absolute value of the slope of G1/S size in generation n vs. generation n+1 is >0.95. Gene copy-number effects increase the regions of parameter space that cause loss of size control (compare with Fig. 3A, where $r_{\mathrm{S/G2/M}} = 1$).

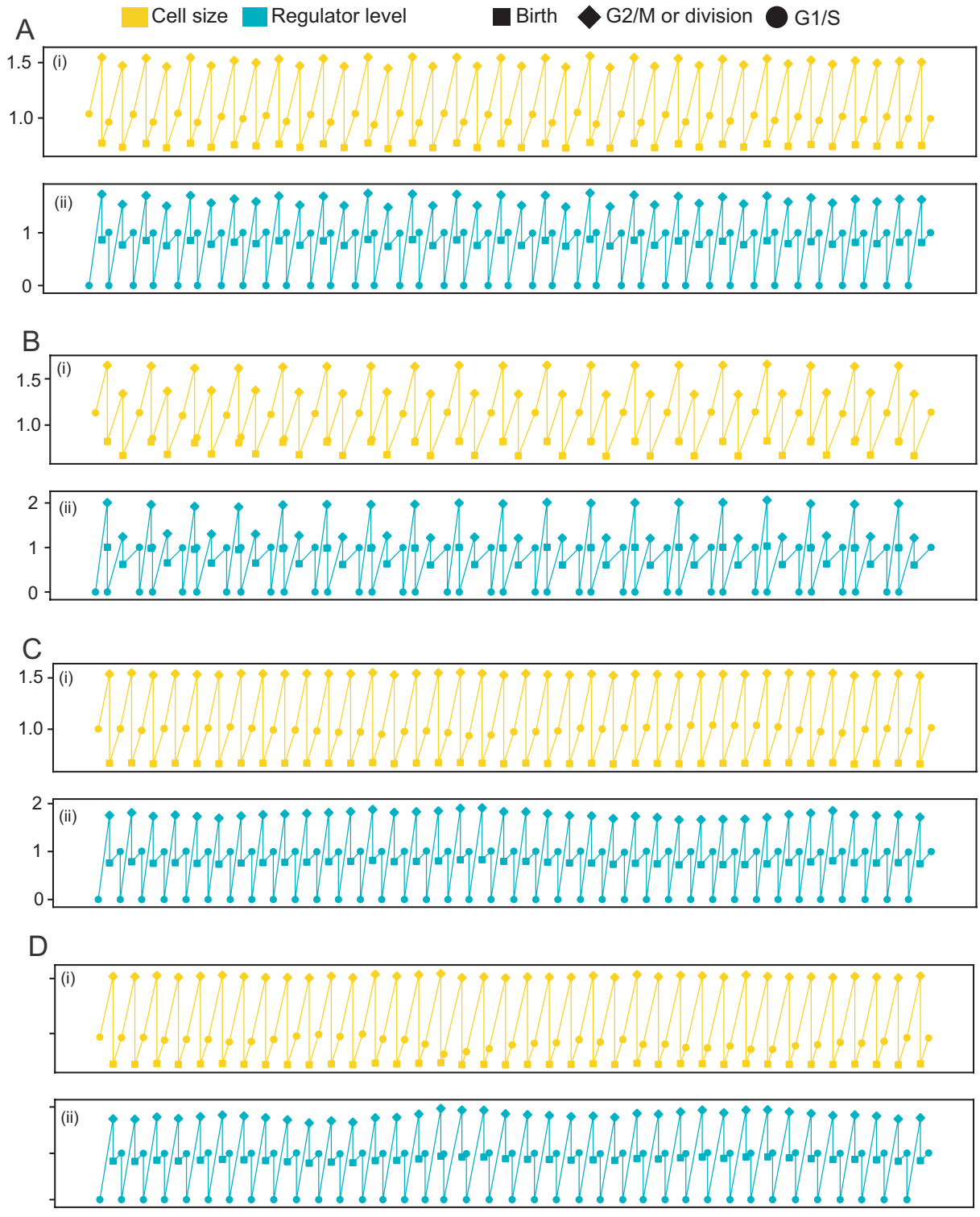
Cell size
Regulator level
Birth
G2/M or division
G1/S
A
(i)
1.5
1.0
(ii)
1
0
B
(i)
1.5
1.0
(ii)
2
1
0
C
(i)
1.5
1.0
(ii)
2
1
0
D
(i)
(ii)

Figure S3: Single-cell trajectories show loss and maintenance of size homeostasis for DnaA-like G1/S two-phase master regulators with gene copy-number production effects. Simulations of single-cell trajectories from Fig. S2. Cells are exponentially growing with G1/S under DnaA-like two-phase master regulator control triggering checkpoint progression at a threshold absolute level ($\lambda_T = 0$) and gene-copy number limited production ($r_{\mathrm{S/G2/M}} = 2$).

(A) Under a strongly size-dependent production rate ($\lambda_c = \lambda_{c,\mathrm{G1}} = \lambda_{c,\mathrm{S/G2/M}} = 3$), S/G2/M adder regulation combined with binary fission ($\sigma = 2$) exhibits size homeostasis when $\tau = 0.55$.

(B) However, size homeostasis is lost when $\tau = 0.4$ with other parameters as in (A); then, G1/S transitions alternate between the beginning (when they are coincident with birth) and the end of the cell cycle.

(C) Regardless of the size dependence of production, and thus even when the production rate is not strongly size-dependent (e.g. $\lambda_c = \lambda_{c,\mathrm{G1}} = \lambda_{c,\mathrm{S/G2/M}} = 1$), critical-size G2/M regulation maintains size homeostasis when $\sigma > 2.1$. Here $\sigma = 2.5$ and $\tau = 0.5$.

(D) However, G1/S size homeostasis is lost when $\sigma \downarrow 2$; here $\sigma = 2.1$ while other parameters are as in (C). G1/S size exhibits long-lived deviations from the average size (compare with (C)), consistent with analytical predictions of a slope between consecutive G1/S sizes ≥ 1.

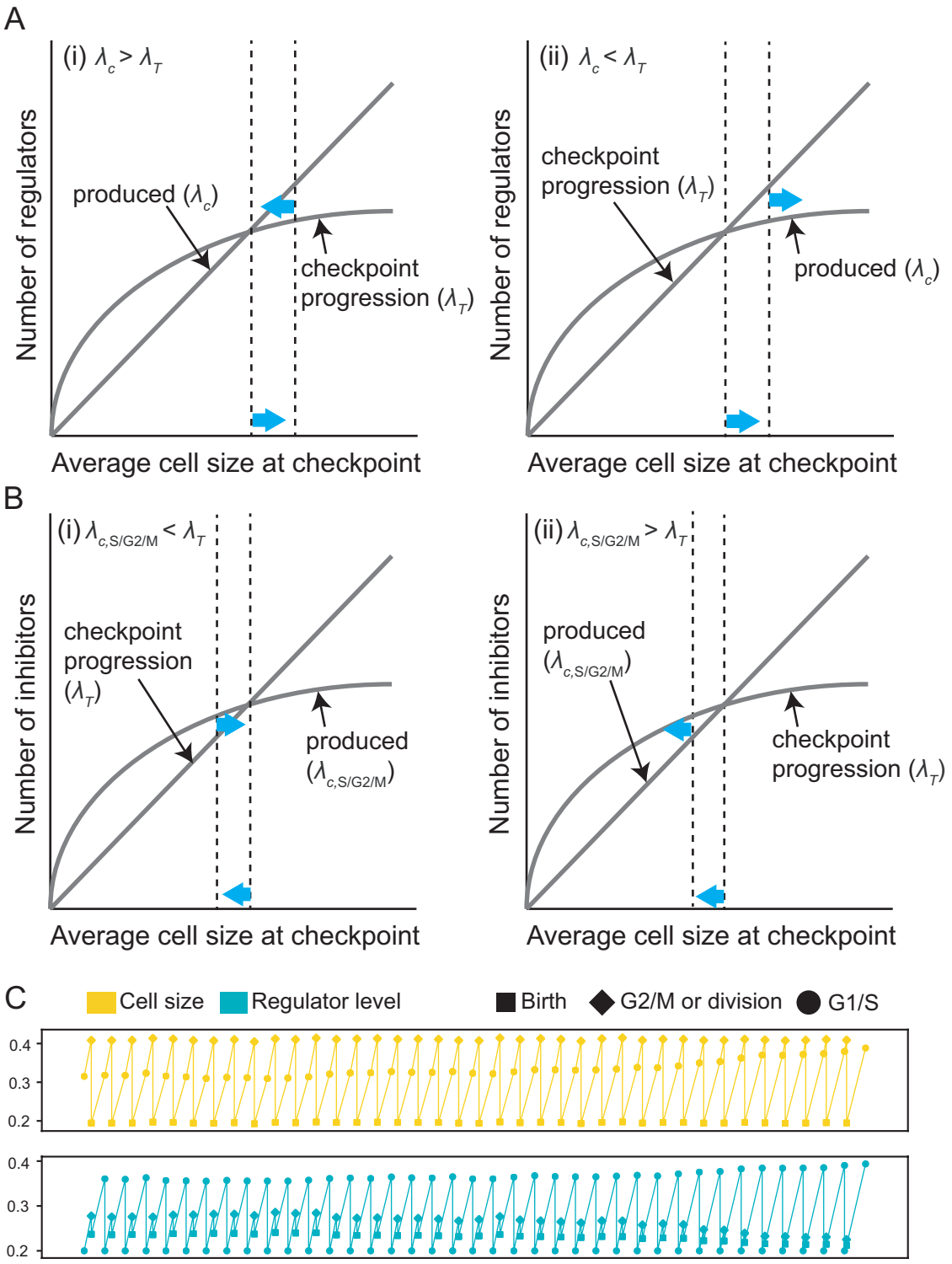

Figure S4: A stable average checkpoint size is required for size homeostasis.

A second condition for cell-size homeostasis is the attainment of a stable average cell size.

(A) For two-phase master regulators with continual size-dependent production rate $\lambda_c = \lambda_{c,\mathrm{G1}} = \lambda_{c,\mathrm{S/G2/M}}$, this condition fails when $\lambda_T > \lambda_c$. Then, positive fluctuations in the average size for checkpoint progression require a surplus of regulator that is not met by the additional amount of regulator produced, so the average checkpoint size increases further, resulting in a loss of stability ((i) vs. (ii)).

(B) For G1/S inhibitor dilutors with a size-dependent production of $\lambda_{c,\mathrm{S/G2/M}}$ through S/G2/M, this condition fails when $\lambda_{c,\mathrm{S/G2/M}} > \lambda_T$. Then, negative fluctuations in the G1/S average size result in the production of less regulator, while the minimum quantity of regulator necessary for checkpoint progression drops but to a lesser extent, so the G1/S average size drops further, resulting in loss of stability ((i) vs. (ii)).

(C) A simulation of single-cell trajectories of G1/S two-phase master regulators with $\lambda_T = 1.0 > \lambda_c = 0.5$, $\tau = 0.6$ and G2/M critical-size regulation shows how G1/S size can diverge quickly from its initial average.

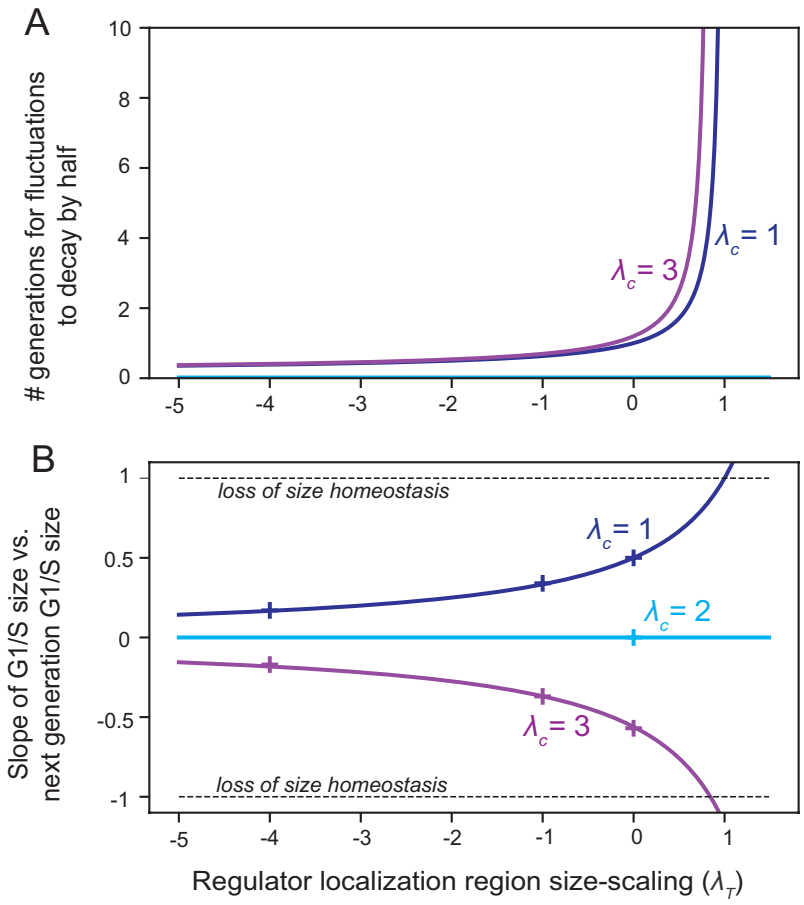

901

902 **Figure S5: DnaA-like two-phase master regulators maximize size-homeostasis**

903 **strength across proliferation scenarios by minimizing the regulator-localization**

904 **region's growth.** As λ_T decreases, the half-lives (A) and the absolute values of slopes

905 between consecutive G1/S sizes (B) decrease for DnaA-like G1/S two-phase master

906 regulators (Eq. 2, Fig. 1G). Here, growth is exponential, $\sigma = 2, \tau = 0.5$, $r_{\mathrm{S/G2/M}} = 1$, and

907 $\lambda_c = \lambda_{c,\mathrm{G1}} = \lambda_{c,\mathrm{S/G2/M}} = 1, 2$, or 3 as indicated. Cross-bars represent simulations with

908 realistic size fluctuations.

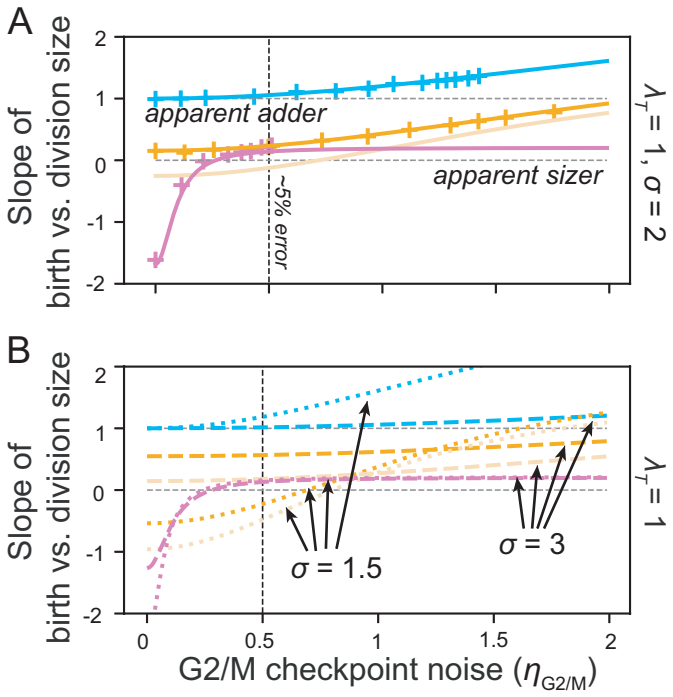

Figure S6: Noisy cell-cycle checkpoints have complex effects on size homeostasis measurements among inhibitor dilutors.

(A) As stated in the main text and Fig. 6D, under binary fission ($\sigma = 2$), $\tau = 0.5$, and $\lambda_T = 1$, inhibitor dilutors with constant production through S/G2/M are relatively weakly affected by G2/M checkpoint noise ($\eta_{G2/M}$) for S/G2/M timer, adder, or near-adder regulation ($f_{S/G2/M} = 2^{0.5}$, 1, or 0.8): typical ~5% errors increase birth size vs. division size slopes by ~5%, assuming a coefficient of variation in G1/S size of ~0.1 and $\eta_{G1/S} = 0$. The response is much stronger for S/G2/M near sizer regulation ($f_{S/G2/M} = 0.1$).

(B) However, as σ decreases, size homeostasis behaviors respond more strongly to G2/M checkpoint noise. In general, among inhibitor dilutors, parameters

affect the size-homeostasis response to noise in a complex manner (Eq. 3, Fig. 1G).

A

Mechanism	Ref.	Predicted l_{G1}	Predicted $l_{S/G2/M}$	Predicted $CV_{G1\ vs.\ S/G2/M}$
(1) G2/M two-phase master regulator with no birth-size dependent production	Fig. 7B	No restriction	-0.3 + 0.4 $l_{G1}(CV_{G1\ vs.\ S/G2/M})^2$	No restriction
(2) G1/S budding yeast-like inhibitor dilutor with a noisy G1/S checkpoint	Fig. 7C	0.4	1.2	1
(3) G2/M two-phase master regulator with gene copy-number limited production	Panel B	0	0.5	No restriction
(4) G2/M two-phase master regulator with production ~cell-size squared	Panel C	No restriction	$l_{G1}(CV_{G1\ vs.\ S/G2/M})^2/4$	No restriction
(5) G1/S two-phase master regulator with a noisy G2/M checkpoint	Panel D	$0.5/l_{S/G2/M}$	>0	$1.4\ l_{S/G2/M}/\sigma_{S/G2/M}$

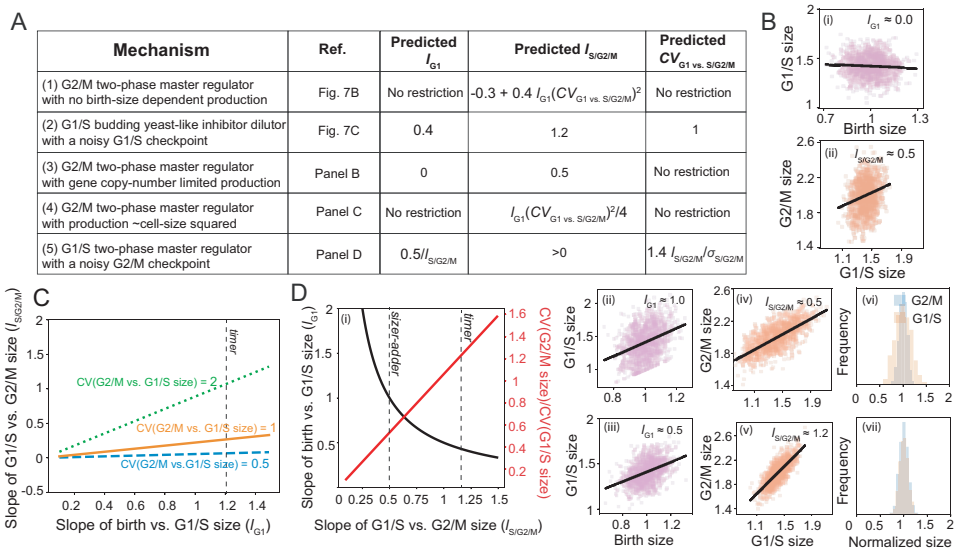

Figure S7: Distinguishing predictions for mechanisms that generate intermediate sizer-adder behavior. At least 5 mechanisms can account for the intermediate sizer-adder behavior observed in *A. thaliana* stem cells. Some of these mechanisms differ in their predictions for: (i) the LRS between birth and G1/S size (l_{G1}); (ii) the LRS between G1/S and G2/M size ($l_{S/G2/M}$); and (iii) the CV(G1/S size)/CV(G2/M size) = $CV_{G1\ vs.\ S/G2/M}$. In all panels, simulations are based on realistic noise levels (CV(G1/S size)≈0.1). Solid black lines in scatter plots correspond to linear regression fits.

(A) Summary table of 5 mechanisms that generate intermediate sizer-adder behavior and their corresponding predictions for l_{G1}, $l_{S/G2/M}$, and $CV_{G1\ vs.\ S/G2/M}$. Mechanisms (1) and (2) are described in the main text and Fig. 7. Mechanisms (3)-(5) are described in (B-D).

(B) Mechanism 3: A G2/M two-phase master regulator triggering G2/M at a threshold level ($\lambda_T = 0$) produced in proportion to cell size ($\lambda_c = \lambda_{c,G1} =$

$\lambda_{c,\mathrm{S/G2/M}} = 1$) with the same birth-size dependence as growth ($\alpha_{c,\mathrm{phase}} = \alpha_g = -0.5$, SI) and gene copy-number limited production ($r_{\mathrm{S/G2/M}} = 2$), with the latter implying that regulator production is not proportional to growth throughout the cell cycle. Predictions are apparent G1/S sizer regulation ($l_{\mathrm{G1}} \approx 0$; top), and apparent sizer-adder regulation over S/G2/M ($l_{\mathrm{S/G2/M}} \approx 0.5$; middle).

(C) Mechanism 4: A G2/M two-phase master regulator triggering G2/M at a threshold level ($\lambda_T = 0$) produced in proportion to cell-size squared ($\lambda_c = \lambda_{c,\mathrm{G1}} = \lambda_{c,\mathrm{S/G2/M}} = 2$) with no gene copy-number effect ($r_{\mathrm{S/G2/M}} = 1$) and the same birth-size dependence as growth ($\alpha_{c,\mathrm{phase}} = \alpha_g = -0.5$, SI). Predictions are similar to mechanism 1 (compare with Fig. 7B). Thus, to discriminate between mechanisms 1 and 4, it would be necessary to measure regulator levels over the cell cycle.

(D) Mechanism 5: A G1/S two-phase master regulator triggering G1/S at a threshold level ($\lambda_T = 0$) produced in proportion to growth ($\lambda_c = \lambda_{c,\mathrm{G1}} = \lambda_{c,\mathrm{S/G2/M}} = 1, r_{\mathrm{S/G2/M}} = 1, \alpha_{c,\mathrm{phase}} = \alpha_g = -0.5$, SI) with noisy supra-sizer S/G2/M regulation (e.g. adder or timer) such that $\beta\eta_{\mathrm{G2/M}} \approx f_{\mathrm{S/G2/M}}/\sigma_{\mathrm{S/G2/M}}$ (SI). (i) Different possible S/G2/M regulatory modes ($f_{\mathrm{S/G2/M}} = l_{\mathrm{S/G2/M}}$; x-axis) predict different apparent G1 size-homeostasis behaviors (l_{G1}; y-axis, left) and $\mathrm{CV}_{\mathrm{G1\ vs.\ S/G2/M}}$ (y-axis; right). (ii-vii) For example, S/G/M intermediate sizer-adder regulation ($l_{\mathrm{S/G2/M}} \approx 0.5$)

predicts $l_{\mathrm{G1}} \approx 1.0$ and $\mathrm{CV}_{\mathrm{G1\ vs.\ S/G2/M}} \approx 0.6$ (top row); S/G2/M timer regulation ($l_{\mathrm{S/G2/M}} \approx 1.2$) predicts $l_{\mathrm{G1}} \approx 0.5$ and $\mathrm{CV}_{\mathrm{G1\ vs.\ S/G2/M}} \approx 1.5$ (bottom row).

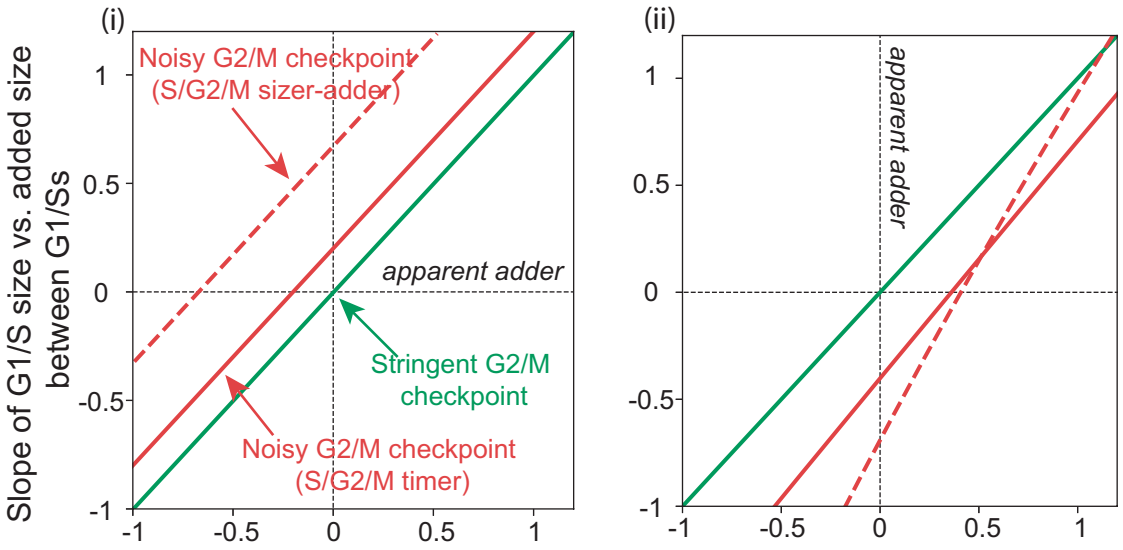

Figure S8: Apparent size-homeostasis behaviors between consecutive G1/Ss and consecutive G2/Ms are identical under stringent checkpoint controls.

The apparent size-homeostasis behaviors between consecutive G2/Ms and consecutive G1/Ss are identical if the cell cycle is controlled by one independently regulated phase with low checkpoint noise (either G1/S or G2/M) (SI). (i) For a G1/S two-phase master regulator combined with an independently regulated S/G2/M phase and realistic noise levels (CV(G1/S size) ≈ 0.1), the same size-homeostasis behavior is observed between birth and division and consecutive G1/Ss when the G2/M checkpoint is stringent (green line); the equality is lost as the G2/M checkpoint noise contributions increases (red lines). Different size homeostasis behaviors were achieved by varying the size dependency of the regulator's production rate (λ_c). (ii) Results are similar for G1/S inhibitor dilutors combined with an independently regulated S/G2/M phase.

STAR Methods

CONTACT FOR RESOURCE SHARING

Further information and requests for resources should be directed to and will be fulfilled by the Lead Contact, Kerwyn Casey Huang (kchuang@stanford.edu).

METHOD DETAILS

Models

We study two classes of regulators, with total intracellular level C, that trigger G1/S or G2/M progression and are produced in a potentially size-dependent manner with negligible degradation. Parameters $\lambda_{c,\mathrm{phase}}$ in phases G1 and S/G2/M determine the cell size (S) dependencies of regulator production $\left(\frac{dC}{dt}\right)$ according to

$$\text{(M1)} \qquad \frac{dC}{dt} = \kappa_{\mathrm{phase}}\, S^{\lambda_{c,\mathrm{phase}}}.$$

Master regulators are produced through one or two phases to trigger G1/S or G2/M progression upon reaching a threshold density $\rho_{\mathrm{checkpoint}}$ within a cellular region that depends on cell size as $\sim S^{\lambda_T}$; degradation to zero then follows (Fig. 1A). Inhibitor dilutors are produced throughout one phase and then diluted out in the subsequent phase to trigger G1/S or G2/M at a minimum threshold density $\rho_{\mathrm{checkpoint}}$, again in an intracellular region that depends on cell size as $\sim S^{\lambda_T}$ (Fig. 1A). G2/M and division are assumed to be coincident. Upon division, cells divide symmetrically ($\sigma = 2$) or asymmetrically ($\sigma \neq 2$) in a ratio 1:($\sigma - 1$) and any regulator that persists is inherited in

992 proportion to daughter cell size (Fig. 1B). Hence, at steady state, the overall fold-size
993 increase is σ, and division-plane positioning is independent of the preceding birth and
994 G1/S sizes. Analyses and simulations assume steady-state population dynamics of one
995 cell type: following each division, only one daughter cell, corresponding to an average
996 portion size of 1 and not $\sigma - 1$, is retained for analyses or simulations. The cellular
997 growth rate $\left(\frac{dS}{dt}\right)$ depends on cell size according to

998 $$\text{(M2)} \qquad \frac{dS}{dt} = \gamma S^{\lambda_g}$$

999 where λ_g determines the growth type (exponential for $\lambda_g = 1$ and linear for $\lambda_g = 0$) and
1000 γ sets the average timescale for growth (Fig. 1C).
1001
1002 Master regulators or inhibitor dilutors are often considered in combination with an
1003 independently regulated S/G2/M or G1 phase: cell size at the end of the phase ($S_{\mathrm{e,phase}}$)
1004 depends on cell size at the beginning of the phase ($S_{\mathrm{i,phase}}$) according to

1005 $$\text{(M3)} \quad S_{\mathrm{e,phase}} = f_{\mathrm{phase}}\, S_{\mathrm{i,phase}} + (\sigma_{\mathrm{phase}} - f_{\mathrm{phase}})\, \mu_{\mathrm{i,phase}},$$

1006 where f_{phase} is the mode of control ($f_{\mathrm{phase}} = 0$, 1, or depends on growth behavior for
1007 "sizer", "adder", or "timer" control, respectively), $\sigma_{\mathrm{phase}} > 1$ is the average fold-size
1008 increase, and $\mu_{\mathrm{i,phase}}$ is the average initial size at steady state (Fig. 1D). The steady-state
1009 fold-size increase over G1 and S/G2/M are related to the fraction of the cell cycle spent
1010 in G1 (τ) by $\sigma_{\mathrm{G1}} \approx \sigma^{\tau}$ and $\sigma_{\mathrm{S/G2/M}} \approx \sigma^{1-\tau}$ because $\sigma_{\mathrm{S/G2/M}} = \sigma/\sigma_{\mathrm{G1}}$. (The approximations

are exact for exponential growth where the cell cycle duration is $\ln\sigma/\gamma$, so $\tau = \frac{T}{\ln\sigma}/\gamma$ if T is the average G1 duration and $\sigma_{\mathrm{G1}} = \frac{\mu_{\mathrm{i,S/G2/M}}}{\mu_{\mathrm{i,G1}}} = e^{\gamma T} = e^{\ln\sigma\,\tau} = \sigma^{\tau}$.) The natural choice of free parameters changes with the control type of the independently regulated phase. For example, for an independently regulated phase under timer control, the natural free parameter is the duration of the phase or the fraction of the cell cycle spent in the phase (τ), whereas for critical size or equivalently sizer control, the natural choice is the average cell size at the transition ($\mu_{\mathrm{e,phase}}$). Regardless of the natural choice, at steady state an equation connecting τ and $\mu_{\mathrm{i,phase}}$ or $\mu_{\mathrm{e,phase}}$ (SI) allows us to work in terms of the parameter τ (or σ_{G1}). Parameter sets that fail to implement cell cycles with two checkpoints on average are then straightforward to exclude by enforcing $0 \leq \tau \leq 1$.

More general analyses in the SI allow growth and production rates to continually depend on cell size at the beginning of the phase, and growth parameters λ_g and γ to differ in G1 vs. S/G2/M.

Analyses

Throughout analyses, linear regression slopes (LRSs) between cell-size variables were derived as follows: scaled cell-size fluctuations at each checkpoint ($\Delta S_{\mathrm{G1/S}} = S_{\mathrm{G1/S}}/\mu_{e,\mathrm{G1}} - 1$ and $\Delta S_{\mathrm{G2/M}} = S_{\mathrm{G2/M}}/\mu_{e,\mathrm{S/G2/M}} - 1$) were expressed in terms of scaled size fluctuations at earlier checkpoints, then only linear terms from a Taylor expansion and

noise terms were retained for analyses because cell-size fluctuations are small (in most measurements, the CV in cell size is ~0.13 (Cadart, 2018; Cadart et al., 2018; Taheri-Araghi et al., 2015; Willis et al., 2016)) and noise terms are comparable in magnitude to cell-size fluctuations (Amir, 2014). Indeed, analytically derived LRSs are in excellent agreement with simulations with realistic noise levels, indicating that the linear approximation is appropriate (Fig. 5,6).

We present two simple examples; the general case is detailed in SI. First we consider a master regulator produced from 0 at G1/S through S/G2/M to trigger G2/M at a threshold density $\rho_{\mathrm{G2/M}}(1 + Z_{\mathrm{G2/M}})$ (where $Z_{\mathrm{G2/M}}$ is the G2/M checkpoint noise with zero average and a standard deviation that corresponds to the CV in the threshold density). The linearized relationship between $\Delta S_{\mathrm{G1/S}}$ and $\Delta S_{\mathrm{G2/M}}$ is found by solving Eqs. M1 and M2 while taking noise in regulator production vs. growth over S/G2/M into account ($Z_{C,\mathrm{S/G2/M}}$), followed by a Taylor expansion,

$$(\mathrm{M4})\quad \Delta S_{\mathrm{G2/M}} = \frac{\sigma_{\mathrm{S/G2/M}}^{\Delta\lambda-1}}{1-\lambda_T\left(\frac{1-\sigma_{\mathrm{S/G2/M}}^{\Delta\lambda-1}}{1-\Delta\lambda}\right)}\left(\Delta S_{\mathrm{G1/S}} + \left(\frac{\sigma_{\mathrm{S/G2/M}}^{1-\Delta\lambda}-1}{1-\Delta\lambda}\right)(Z_{\mathrm{G2/M}} + Z_{C,\mathrm{S/G2/M}})\right)$$

$$+ \text{higher order terms}$$

where $\Delta\lambda = \lambda_g - \lambda_{c,\mathrm{S/G2/M}}$ and $Z_{C,\mathrm{S/G2/M}}$ is a zero-average random variable. By definition, the LRS between G1/S and G2/M sizes is

(M5) $$\frac{\mathbf{E}[(S_{\mathrm{G2/M}} - \mu_{e,\mathrm{S/G2/M}})(S_{\mathrm{G1/S}} - \mu_{e,\mathrm{G1}})]}{\mathbf{E}[(S_{\mathrm{G1/S}} - \mu_{e,\mathrm{G1}})^2]} = \frac{\sigma_{\mathrm{S/G2/M}}\,\mathbf{E}[\Delta S_{\mathrm{G2/M}} \Delta S_{\mathrm{G1/S}}]}{\mathbf{E}[(\Delta S_{\mathrm{G1/S}})^2]}$$

where $\mathbf{E}[\cdot]$ denotes the expected value (average; SI). So, the LRS is computed by multiplying Eq. M4 by $\sigma_{\mathrm{S/G2/M}} \Delta S_{\mathrm{G1/S}}$, taking averages of each side of the equation, and dividing by $\mathbf{E}[(\Delta S_{\mathrm{G1/S}})^2]$. Since G1/S size fluctuations ($\Delta S_{\mathrm{G1/S}}$) are independent of noise in the subsequent G2/M threshold density ($Z_{\mathrm{G2/M}}$) and regulator dynamics compared with growth over S/G2/M ($Z_{C,\mathrm{S/G2/M}}$), upon taking averages, the noise terms disappear. Thus, the LRS between G1/S and G2/M sizes is $\frac{\sigma_{\mathrm{S/G2/M}}^{\Delta\lambda - 1}}{1 - \lambda_T \left(\frac{1 - \sigma_{\mathrm{S/G2/M}}^{\Delta\lambda - 1}}{1 - \Delta\lambda} \right)}$.

Second, we consider independently regulated phases. From Eq. M3, taking checkpoint noise into account, we have

$$S_{\mathrm{e,phase}} = f_{\mathrm{phase}}\, S_{\mathrm{i,phase}} + (1 - \frac{f_{\mathrm{phase}}}{\sigma_{\mathrm{phase}}} + \beta\, Z_{\mathrm{checkpoint}})\, \sigma_{\mathrm{phase}}\, \mu_{\mathrm{i,phase}},$$

where the zero-average checkpoint noise term $\beta\, Z_{\mathrm{checkpoint}}$ with $\beta = 1 - \frac{f_{\mathrm{phase}}}{\sigma_{\mathrm{phase}}} + \frac{f_{\mathrm{phase}}}{\sigma_{\mathrm{phase}}} \ln f_{\mathrm{phase}}$ ensures that the standard deviation of $Z_{\mathrm{checkpoint}}$ corresponds to the CV in either the critical size (sizer, $f_{\mathrm{phase}} = 0$), critical increment (adder, $f_{\mathrm{phase}} = 1$), or timer regulation ($f_{\mathrm{phase}} = \sigma_{\mathrm{phase}}$; see below) (SI). Rearrangement gives

$$\Delta S_{\mathrm{e,phase}} = \frac{f_{\mathrm{phase}}}{\sigma_{\mathrm{phase}}} \Delta S_{\mathrm{i,phase}} + \beta\, Z_{\mathrm{checkpoint}}.$$

The LRS between sizes at the beginning vs. end of the phase is computed according to Eq. M5 to give f_{phase}.

Regardless of the nature of cell cycle control, the LRS between scaled fluctuations in a phase's duration and scaled size fluctuations at the beginning of the phase is

$$\frac{1-\lambda_g}{\sigma_{\text{phase}}-\sigma_{\text{phase}}^{\lambda_g}}\left(l_{\text{phase}}-\sigma_{\text{phase}}^{\lambda_g}\right)$$

where l_{phase} is the LRS between cell size at the beginning vs. cell size at the end of the phase (SI). This slope must be zero for independently regulated timer phases, thus, for timer regulation, $l_{\text{phase}} = f_{\text{phase}} = \sigma_{\text{phase}}^{\lambda_g}$.

Other LRSs were derived similarly but often the dependence of size fluctuations on checkpoint noise terms in preceding phases causes noise to affect size homeostasis behaviors (SI). Then, noise manifests through the parameters

$$\eta_{\text{checkpoint}} = \frac{\text{Noise in the transition's checkpoint mechanism}}{\text{CV in G1/S size}}$$

$$= \frac{\text{Standard deviation in } Z_{\text{checkpoint}}}{\text{CV in G1/S size}}$$

(SI). Importantly, throughout analyses, no assumptions were made about the distributions of $Z_{\text{G1/S}}$, $Z_{C,\text{G1}}$, $Z_{\text{G2/M}}$, and $Z_{C,\text{S/G2/M}}$ beyond the values of their standard

deviations, indicating that, for small fluctuations in cell size, further properties of the distributions (e.g. skewness) have no effect on size homeostasis behaviors.

General expressions for size homeostasis behaviors

Applying the methods above, we derived LRSs between birth and division sizes and other statistics for the general model. Here we summarize the results presented in Fig. 1G, assuming exponential growth ($\lambda_g = 1$) and a persistent size-dependent production through both phases ($\lambda_c = \lambda_{c,\mathrm{G1}} = \lambda_{c,\mathrm{S/G2/M}}$) for two-phase master regulators. These expressions frame the combined generic effects of regulator production, regulator localization, gene copy-number effects, G1 duration, noise, division mode, and mode of control of the independently regulated phase on size-homeostasis statistics. The effects of deviations in growth patterns are detailed in SI.

For CDK-cyclin- or FtsZ-like G2/M two-phase master regulators, the LRS of birth size vs. birth size in the subsequent generation is

$$(1) \qquad \frac{\sigma^{-\lambda_c}\, r_{\mathrm{S/G2/M}}^{-1} \;+\; {\sigma_{\mathrm{S/G2/M}}}^{-\lambda_c}\left(1 - r_{\mathrm{S/G2/M}}^{-1}\right) l_{\mathrm{G1}}/\sigma_{\mathrm{G1}}}{1 - \frac{\lambda_T}{\lambda_c}\left(1 - {\sigma_{\mathrm{S/G2/M}}}^{-\lambda_c} + r_{\mathrm{S/G2/M}}^{-1}\left({\sigma_{\mathrm{S/G2/M}}}^{-\lambda_c} - \sigma^{-\lambda_c}\right)\right)}$$

where the LRS of birth size vs. G1/S size $l_{\mathrm{G1}} = f_{\mathrm{G1}}$ when G1 is independently regulated (from section **Analyses**), and for exponential growth $\sigma_{\mathrm{S/G2/M}} = \sigma^{1-\tau}$, $\sigma_{\mathrm{G1}} = \sigma^{\tau}$. Noise terms do not affect this statistic. A slope of $1/\sigma$ (recovered from Eq. 1 when $\lambda_T = 0, \lambda_c =$

1, and $r_{\mathrm{S/G2/M}} = 1$) corresponds to apparent adder behavior (a LRS of 1 for birth size vs. division size, because birth size in the subsequent generation = division size/σ), while apparent sizer behavior corresponds to a slope of 0. If G1 is independently regulated with relatively stringent control of G1/S (relative typical errors < $f_{\mathrm{G1}}/\sigma_{G1}$), then the LRS between consecutive G1/S sizes equals the LRS between consecutive birth (or equivalently G2/M) sizes (Fig. S8; SI).

A DnaA-like G1/S two-phase master regulator with an independently regulated S/G2/M phase produces an LRS of birth size vs. birth size in the subsequent generation of

$$(2) \quad \frac{r_{\mathrm{S/G2/M}}\sigma^{-1}\dfrac{\left(\frac{f_{\mathrm{S/G2/M}}}{\sigma_{\mathrm{S/G2/M}}}\right)^2}{\left(\frac{f_{\mathrm{S/G2/M}}}{\sigma_{\mathrm{S/G2/M}}}\right)^2 + \beta^2\eta_{\mathrm{G2/M}}^2} + \frac{f_{\mathrm{S/G2/M}}}{\sigma_{\mathrm{S/G2/M}}}\left({\sigma_{\mathrm{G1}}}^{-\lambda_c} - r_{\mathrm{S/G2/M}}\sigma^{-1}{\sigma_{\mathrm{S/G2/M}}}^{\lambda_c}\right)}{1 - \frac{\lambda_T}{\lambda_c}\left(1 - {\sigma_{\mathrm{G1}}}^{-\lambda_c} + r_{\mathrm{S/G2/M}}\sigma^{-1}\left({\sigma_{\mathrm{S/G2/M}}}^{\lambda_c} - 1\right)\right)}$$

where $\beta = 1 - \frac{f_{\mathrm{S/G2/M}}}{\sigma_{\mathrm{S/G2/M}}}(1 - \ln f_{\mathrm{S/G2/M}})$. Independent regulation of S/G2/M implies the LRS of G1/S vs. division sizes is $f_{\mathrm{S/G2/M}}$ (from section **Analyses**), and a low noise contribution from the G2/M checkpoint ($\beta\,\eta_{\mathrm{G2/M}} \ll f_{\mathrm{S/G2/M}}/\sigma_{\mathrm{S/G2/M}}$) produces an LRS of G1/S size vs. G1/S size in the subsequent generation identical to Eq. 2 (SI). Regardless of noise, the LRS of birth size vs. G1/S size is Eq. $2 \times \sigma_{\mathrm{G1}}\frac{f_{\mathrm{S/G2/M}}}{\sigma_{\mathrm{S/G2/M}}}$ (SI).

G1/S inhibitor dilutors combined with independent regulation of S/G2/M produce an LRS of birth size vs. birth size in the subsequent generation of

$$\sigma^{-1}\left(\frac{\left(\frac{f_{\mathrm{S/G2/M}}}{\sigma_{\mathrm{S/G2/M}}}\right)^2}{\left(\frac{f_{\mathrm{S/G2/M}}}{\sigma_{\mathrm{S/G2/M}}}\right)^2+\beta^2\eta_{\mathrm{G2/M}}^2}\left(1-\frac{\lambda_{c,\mathrm{S/G2/M}}}{\lambda_T}\frac{\sigma-1}{{\sigma_{\mathrm{S/G2/M}}}^{\lambda_{c,\mathrm{S/G2/M}}}-1}-\frac{\eta_{\mathrm{G1/S}}^2}{{\lambda_T}^2}\right)+\frac{f_{\mathrm{S/G2/M}}}{\sigma_{\mathrm{S/G2/M}}}\frac{\lambda_{c,\mathrm{S/G2/M}}}{\lambda_T}\frac{{\sigma_{\mathrm{S/G2/M}}}^{\lambda_{c,\mathrm{S/G2/M}}}(\sigma-1)}{{\sigma_{\mathrm{S/G2/M}}}^{\lambda_{c,\mathrm{S/G2/M}}}-1}\right). \quad (3)$$

Again, $f_{\mathrm{S/G2/M}}$ is the LRS between G1/S size vs. division size, and a low noise contribution from the G2/M checkpoint ($\beta\,\eta_{\mathrm{G2/M}} \ll f_{\mathrm{S/G2/M}}/\sigma_{\mathrm{S/G2/M}}$) produces an LRS between G1/S size vs. G1/S size in the subsequent generation equal to Eq. 3. Regardless of noise, the LRS of birth size vs. G1/S size is Eq. 3 $\times\ \sigma_{\mathrm{G1}}\frac{f_{\mathrm{S/G2/M}}}{\sigma_{\mathrm{S/G2/M}}}$ (SI). The expressions for G2/M inhibitor dilutors are analogous (SI). In Eq. 3, a slope of $1/\sigma$ corresponding to apparent adder behavior is recovered for the default Whi5 parameters ($f_{\mathrm{S/G2/M}} = \sigma_{\mathrm{S/G2/M}}$ for S/G2/M timer regulation, $\lambda_T = 1, \lambda_c = 0$) when cell cycle checkpoint noise contributions are low compared with other noise sources ($\eta_{\mathrm{G1}}, \eta_{\mathrm{G2/M}} \ll 1$) and regardless of σ or τ.

Conditions for the loss of size homeostasis

We specify two conditions under which size homeostasis is lost. These conditions are necessary for size homeostasis but may not be sufficient. The first condition is that

fluctuations away from the average size at G1/S and G2/M must not diverge. Derivations similar to those in section **Analyses** led to first-order expressions connecting size fluctuations at G1/S and G2/M in consecutive cell cycles

$$\Delta S'_{\mathrm{G1/S}} = \alpha_{\mathrm{G1}} \Delta S_{\mathrm{G1/S}} + \text{noise terms}$$

$$\Delta S'_{\mathrm{G2/M}} = \alpha_{\mathrm{S/G2/M}} \Delta S_{\mathrm{G2/M}} + \text{noise terms}$$

where ' denotes the subsequent cell cycle, and α_{G1} and $\alpha_{\mathrm{S/G2/M}}$ are functions of model parameters (SI). Even in the absence of noise, fluctuations diverge when $|\alpha_{\mathrm{G1}}| \geq 1$ or $|\alpha_{\mathrm{S/G2/M}}| \geq 1$ for G1/S or G2/M, respectively (Fig. 2A). The colored regions of Fig. 3A and 4A show where $|\alpha_{\mathrm{G1}}| \geq 1$ or $|\alpha_{\mathrm{S/G2/M}}| \geq 1$ for the parameters specified in each plot. Simulations of single-cell trajectories with $|\alpha_{\mathrm{G1}}| \approx 1$ and $|\alpha_{\mathrm{S/G2/M}}| \approx 1$, i.e. close to the boundary of size homeostasis, show that size homeostasis is compromised (Fig. 2B, 3B, 4B), supporting our analyses.

The second condition is that the average G1/S and G2/M cell sizes are stable non-zero values. The average cell sizes at a checkpoint are determined by the requirement that the number of regulators for checkpoint progression is equal to the number of regulators produced. For CDK1-cyclin- or FtsZ-like G2/M two-phase master regulators, this relation gives

$$\rho_{\mathrm{G2/M}}\, {\mu_{\mathrm{G2/M}}}^{\lambda_T} = \frac{\kappa_{G1}}{\gamma} \frac{{\sigma_{\mathrm{S/G2/M}}}^{-\lambda_c} - \sigma^{-\lambda_c} + r_{\mathrm{S/G2/M}}(1 - {\sigma_{\mathrm{S/G2/M}}}^{-\lambda_c})}{\lambda_c} {\mu_{\mathrm{G2/M}}}^{\lambda_c} \rightarrow$$

$$\frac{\kappa_{G1}}{\gamma} (\ln \sigma_{\mathrm{S/G2/M}}(r_{\mathrm{S/G2/M}} - 1) + \ln\sigma) {\mu_{\mathrm{G2/M}}}^{\lambda_c} \text{ as } \lambda_c \rightarrow 0$$

where $\rho_{\mathrm{G2/M}}$ is the threshold density for G2/M progression (SI). In the admissible parameter range ($r_{\mathrm{S/G2/M}} \geq 1, \sigma > \sigma_{\mathrm{S/G2/M}} > 1$), there is a stable positive solution for $\mu_{\mathrm{G2/M}}$ if and only if $\lambda_T < \lambda_c$. When this condition is not satisfied, positive fluctuations in the average size for checkpoint progression require a surplus of regulator that is not met by the additional amount of regulator produced, so the average checkpoint size increases further resulting in a loss of stability (Fig. S4A). For DnaA-like two-phase master regulators, we similarly have

$$\rho_{\mathrm{G1/S}}\,{\mu_{\mathrm{G1/S}}}^{\lambda_T} = \frac{\kappa_{G1}}{\gamma}\,\frac{r_{\mathrm{S/G2/M}}\,\sigma^{-1}\left({\sigma_{\mathrm{S/G2/M}}}^{\lambda_c} - 1\right) + \,1 - {\sigma_{\mathrm{G1}}}^{-\lambda_c}}{\lambda_c}\,{\mu_{\mathrm{G1/S}}}^{\lambda_c}$$

which results in the same condition $\lambda_T < \lambda_c$. for stable non-zero average G1/S sizes. By contrast, the equivalent expression for G1/S inhibitor dilutors,

$$\rho_{\mathrm{G1/S}}\,{\mu_{\mathrm{G1/S}}}^{\lambda_T} = \frac{\kappa_{\mathrm{S/G2/M}}}{\gamma}\,\frac{{\sigma_{\mathrm{S/G2/M}}}^{\lambda_{c,\mathrm{S/G2/M}}-1}}{\lambda_{c,\mathrm{S/G2/M}}\,(\sigma-1)}\,{\mu_{\mathrm{G1/S}}}^{\lambda_{c,\mathrm{S/G2/M}}},$$

has stable non-zero average G1/S sizes if and only if $\lambda_{c,\mathrm{S/G2/M}} < \lambda_T$. If this condition is not met, negative fluctuations in the G1/S average size result in the production of less regulator, but the minimum quantity of regulator necessary for checkpoint progression drops to a lesser extent, so the G1/S average size drops further, resulting in loss of stability (Fig. S4B). In some instances, both the first condition that fluctuations away from the average size do not diverge and the second condition that average sizes are stable fail simultaneously (e.g. the limiting scenario in Fig. 2B); in other instances, the first condition fails while the second condition remains satisfied (e.g. the limiting

scenario in Fig. 3B). In any case, whether the control of cell size deteriorates or is maintained as λ_T approaches λ_c or $\lambda_{c,\mathrm{S/G2/M}}$ is determined by whether the absolute value of the slope in Eqs. 1—3 is above or approaches 1.

Simulations

Cells were initialized to the steady-state birth size and regulator level plus noise. Then, cell sizes and regulator levels at G1/S and G2/M were simulated with 2 noise terms per phase according to the differential equations in Eq. M1,M2 until the criterion for checkpoint progression was met. Checkpoint progression triggered regulator degradation and changes in parameters appropriate for the subsequent phase according to the specific model being simulated (e.g. G1/S inhibitor dilutor). At the beginning of each phase, a zero-average Gaussian random variable ($Z_{\mathrm{checkpoint}}$) perturbed the level of regulator to represent noise in regulator production, while another zero-average Gaussian random variable ($Z_{C,\mathrm{phase}}$) perturbed the criterion for checkpoint progression; as described in the Analyses section, the standard deviation of $Z_{\mathrm{checkpoint}}$ was set to the CV of the criterion for checkpoint progression. Upon G2/M, division followed immediately and the regulator level and cell size at birth of the retained daughter in the next generation were

$$C_b' = C_{\mathrm{G2/M}}/\sigma, \qquad S_b' = S_{\mathrm{G2/M}}/\sigma$$

where no noise in division was assumed. Cells were simulated for at least 500 generations until steady states were reached.

References

Amir, A. (2014). Cell size regulation in bacteria. Phys Rev Lett *112*, 208102.

Barber, F., Ho, P.Y., Murray, A.W., and Amir, A. (2017). Details matter: noise and model structure set the relationship between cell size and cell cycle timing. Front Cell Dev Biol *5*.

Cadart, C. (2018). Personal communication.

Cadart, C., Monnier, S., Grilli, J., Attia, R., Terriac, E., Baum, B., Cosentino-Lagomarsino, M., and Piel, M. (2018). Size control in mammalian cells involves modulation of both growth rate and cell cycle duration. Nat Commun *9*, 3275.

Campos, M., Surovtsev, I.V., Kato, S., Paintdakhi, A., Beltran, B., Ebmeier, S.E., and Jacobs-Wagner, C. (2014). A constant size extension drives bacterial cell size homeostasis. Cell *159*, 1433-1446.

Chandler-Brown, D., Schmoller, K.M., Winetraub, Y., and Skotheim, J.M. (2017). The adder phenomenon emerges from independent control of pre- and post-start phases of the budding yeast cell cycle. Curr Biol *27*, 2774—2783.

Coudreuse, D., and Nurse, P. (2010). Driving the cell cycle with a minimal CDK control network. Nature *468*, 1074-1079.

Cross, F.R. (1988). DAF1, a mutant gene affecting size control, pheromone arrest, and cell cycle kinetics of *Saccharomyces cerevisiae*. Mol Cell Biol *8*, 4675—4684.

Dewitte, W., Riou-Khamlichi, C., Scofield, S., Healy, J.M., Jacqmard, A., Kilby, N.J., and Murray, J.A. (2003). Altered cell cycle distribution, hyperplasia, and inhibited differentiation in Arabidopsis caused by the D-type cyclin CYCD3. Plant Cell *15*, 79-92.

Di Talia, S., Skotheim, J.M., Bean, J.M., Siggia, E.D., and Cross, F.R. (2007). The effects of molecular noise and size control on variability in the budding yeast cell cycle. Nature *448*, 947-951.

Eun, Y.-J., Ho, P.-Y., Kim, M., LaRussa, S., Robert, L., Renner, L.D., Schmid, A., Garner, E., and Amir, A. (2018). Archaeal cells share common size control with bacteria despite noisier growth and division. Nat Microbiol *3*, 148—154.

Facchetti, G., Knapp, B., Flor-Parra, I., Chang, F., and Howard, M. (2019). Reprogramming cdr2-dependent geometry-based cell size control in fission yeast. Curr Biol *29*, 350–358.

Fantes, P.A. (1977). Control of cell size and cycle time in *Schizosaccharomyces pombe*. J Cell Sci *24*, 51-67.

Ginzberg, M.B., Chang, N., D'Souza, H., Patel, N., Kafri, R., and Kirschner, M.W. (2018). Cell size sensing in animal cells coordinates anabolic growth rates and cell cycle progression to maintain cell size uniformity. ELife *11*, e26957.

Grilli, J., Cadart, C., Micali, G., Osella, M., and Lagomarsino, M.C. (2018). The empirical fluctuation pattern of *E. coli* division control. Front Microbiol *9*, 1541.

Grilli, J., Osella, M., Kennard, A.S., and Lagomarsino, M.C. (2017). Relevant parameters in models of cell division control. Phys Rev E *95*, 032411.
Harashima, H., Dissmeyer, N., and Schnittger, A. (2013). Cell cycle control across the eukaryotic kingdom. Trends in Cell Biology *23*, 345-356.
Harashima, H., and Sugimoto, K. (2016). Integration of developmental and environmental signals into cell proliferation and differentiation through RETINOBLASTOMA-RELATED 1. Curr Opin Plant Biol *29*, 95–103.
Heldt, F.S., Lunstone, R., Tyson, J.J., and Novák, B. (2018). Dilution and titration of cell-cycle regulators may control cell size in budding yeast. PLOS Comput Biol *14*, e1006548.
Ho, P.-Y., and Amir, A. (2015). Simultaneous regulation of cell size and chromosome replication in bacteria. Front Microbiol *6*, 662.
Hochegger, H., Takeda, S., and Hunt, T. (2008). Cyclin-dependent kinases and cell-cycle transitions: does one fit all? Nat Rev Mol Cell Biol *9*, 910–916.
Jones, A.R., Forero-Vargas, M., Withers, S.P., Smith, R.S., Traas, J., Dewitte, W., and Murray, J.A.H. (2017). Cell-size dependent progression of the cell cycle creates homeostasis and flexibility of plant cell size. Nat Commun *8*, 15060.
Keifenheim, D., Sun, X., D'Souza, E., Ohira, M.J., Magner, M., Mayhew, M.B., Marguerat, S., and Rhind, N. (2017). Size-dependent expression of the mitotic activator Cdc25 suggests a mechanism of size control in fission yeast. Curr Biol *27*, 1491—1497.
Lin, J., and Amir, A. (2018). Homeostasis of protein and mRNA concentrations in growing cells. Nat Commun *9*, 4496.
Logsdon, M.M., Ho, P.Y., Papavinasasundaram, K., Richardson, K., Cokol, M., Sassetti, C.M., Amir, A., and Aldridge, B.B. (2017). A parallel adder coordinates mycobacterial cell-cycle progression and cell-size homeostasis in the context of asymmetric growth and organization. Curr Biol *27*, 3367—3374.
Micali, G., Grilli, J., Marchi, J., Osella, M., and Cosentino Lagomarsino, M. (2018a). Dissecting the control mechanisms for DNA replication and cell division in *E. coli*. Cell Rep *25*, 761.
Micali, G., Grilli, J., Osella, M., and Lagomarsino, M.C. (2018b). Concurrent processes set E. coli cell division. Sci Adv *4*, eaau3324.
Newman, J.R., Ghaemmaghami, S., Ihmels, J., Breslow, D.K., Noble, M., DeRisi, J.L., and Weissman, J.S. (2006). Single-cell proteomic analysis of *S. cerevisiae* reveals the architecture of biological noise. Nature *441*, 840—846.
Nordholt, N., van Heerden, J.H., and Bruggeman, F.J. (2019). Growth-rate and protein-synthesis dynamics of single Bacillus subtilis cells along their cell-cycle. bioRxiv.
Osella, M., Nugent, E., and Cosentino Lagomarsino, M. (2014). Concerted control of *Escherichia coli* cell division. Proc Natl Acad Sci USA *111*, 3431-3435.
Padovan-Merhard, O., Nair, G.P., Biaesch, A.G., Mayer, A., Scarfone, S., Foley, S.W., Wu, A.R., Churchman, L.S., Singh, A., and Raj, A. (2015). Single mammalian cells

compensate for differences in cellular volume and DNA copy number through independent global transcriptional mechanisms. Mol Cell *58*, 339—352.
Pan, K.Z., Saunders, T.E., Flor-Parra, I., Howard, M., and Chang, F. (2014). Cortical regulation of cell size by a sizer cdr2p. eLife *3*.
Patterson, J.O., Rees, P., and Nurse, P. (2019). Noisy cell-size correlated expression of Cyclin B drives probabilistic cell-size homeostasis in fission yeast. Curr Biol *29*, 1379–1386.
Schmoller, K.M., and Skotheim, J.M. (2015). The biosynthetic basis of cell size control. Trends Cell Biol *25*, 793-802.
Schmoller, K.M., Turner, J.J., Koivomagi, M., and Skotheim, J.M. (2015). Dilution of the cell cycle inhibitor Whi5 controls budding-yeast cell size. Nature *526*, 268-272.
Scofield, S., Jones, A., and Murray, J.A.H. (2014). The plant cell cycle in context. J Exp Bot *65*, 2557–2562.
Sekar, K., Rusconi, R., Sauls, J.T., Fuhrer, T., Noor, E., Nguyen, J., Fernandez, V.I., Buffing, M.F., Berney, M., Jun, S., *et al.* (2018). Synthesis and degradation of FtsZ quantitatively predict the first cell division in starved bacteria. Mol Syst Biol *14*, e8623.
Shi, H., Colavin, A., Bigos, M., Tropini, C., Monds, R.D., and Huang, K.C. (2017). Deep phenotypic mapping of bacterial cytoskeletal mutants reveals physiological robustness to cell size. Curr Biol *27*, 3419—3429.
Si, F., Treut, G.L., Sauls, J.T., Vadia, S., Levin, P.A., and Jun, S. (2019). Mechanistic origin of cell-size control and homeostasis in bacteria. Curr Biol *29*, 1–11.
Soifer, I., Robert, L., and Amir, A. (2016). Single-cell analysis of growth in budding yeast and bacteria reveals a common size regulation strategy. Curr Biol *26*, 356-361.
Taheri-Araghi, S., Bradde, S., Sauls, J.T., Hill, N.S., Levin, P.A., Paulsson, J., Vergassola, M., and Jun, S. (2015). Cell-size control and homeostasis in bacteria. Curr Biol *25*, 385-391.
Turner, J.J., Ewald, J.C., and Skotheim, J.M. (2012). Cell size control in yeast. Curr Biol *22*, 350-359.
Varsano, G., Wang, Y., and Wu, M. (2017). Probing Mammalian Cell Size Homeostasis by Channel-Assisted Cell Reshaping. Cell Rep *20*, 397—410.
Wallden, M., Fange, D., Lundius, E.G., Baltekin, Ö., and Elf, J. (2016). The synchronization of replication and division cycles in individual *E. coli* cells. Cell *166*, 729-739.
Wang, P., Robert, L., Pelletier, J., Dang, W.L., Taddei, F., Wright, A., and Jun, S. (2010). Robust growth of *Escherichia coli*. Curr Biol *20*, 1099-1103.
Willis, L., and Huang, K. (2017). Sizing-up the bacterial cell cycle. Nat Rev Microbiol *15*, 606–620.
Willis, L., Refahi, Y., Wightman, R., Landrein, B., Teles, J., Huang, K.C., Meyerowitz, E.M., and Jonsson, H. (2016). Cell size and growth regulation in the Arabidopsis thaliana apical stem cell niche. Proc Natl Acad Sci U S A *113*, E8238-E8246.

1310